Supporting Online Material for

Out of Tibet: Pliocene Woolly Rhino Suggests High-Plateau Origin of Ice Age Megaherbivores

Tao Deng, Xiaoming Wang,* Mikael Fortelius, Qiang Li, Yang Wang, Zhijie J. Tseng, Gary T. Takeuchi, Joel E. Saylor, Laura K. Säilä, Guangpu Xie

*To whom correspondence should be addressed. E-mail: xwang@nhm.org

This PDF file includes:

SOM Text
Figs. S1 to S13
Tables S1 to S8
References (*25–130*)

Geologic setting of Zanda Basin. Zanda Basin is a late Miocene through Pleistocene pull-apart sag basin (Fig. S1) located just north of the high Himalayan ridgecrest in the west-central part of the orogen (~32° N, 82° E; elevation 3,700-4,500 m). It lies between the South Tibetan Detachment System (STDS) to the southwest, and the Indus Suture to the northeast and the Gurla Mandhata and Qusum (Leo Pargil) metamorphic core complexes to the southeast and northwest, respectively. The STDS is an early-mid Miocene (*25*) series of north-dipping, low-angle, top-to-the-north normal faults which place low-grade Paleozoic-Mesozoic metasedimentary rocks on high-grade gneisses and granites of the Greater Himalayan sequence. In the Zanda Basin region the Oligo-Miocene Great Counter Thrust, a south-dipping, top-to-the-north thrust system, modifies the Indus Suture. The age of exhumation of the Gurla Mandhata and Qusum (Leo Pargil) metamorphic core complexes has been defined by ^{40}Ar/^{39}Ar analysis of micas to be ~9 Ma (*26*) or 14-16 Ma (*27*), respectively. The axis of the basin is approximately northwest-southeast; parallel to the general arc of the Himalaya. The current outcrop extent of the basin fill is >9,000 km^2.

The sedimentary basin fill is undisturbed and lies in angular or buttress unconformity with the underlying deformed Tethyan Sedimentary Sequence (TSS) strata. After deposition, incision by the Langqên Zangbo (Sutlej) River exposed the entire basin fill.

The basin fill consists of approximately 800 m of fluvial, lacustrine, eolian and alluvial fan deposits. The lower part of the section consists of approximately 200 m of trough cross-bedded sands and well-organized, imbricated, pebble to cobble conglomerate. Associated sedimentary structures include stacked, 3-4 meter sand-gravel filled channel and longitudinal bar.

We interpret these features as fluvial deposits laid down by large-scale rivers ancestral to the Sutlej or Indus based on provenance and paleocurrent orientation data (*28*). Interbedded fine-grained sand and silt horizons showing extensive soft-sediment deformation and containing abundant mammal, gastropod and plant macrofossils are interpreted as marshy bog or overbank deposits within a low-gradient fluvial setting. The middle unit (approximately 250 m) consists of an upward coarsening succession of lacustrine progradational parasequences. Individual parasequences are up to 17 m thick and range between profundal lacustrine claystones and deltaic and wave-worked sediments, including evidence of occasional desiccation. The top 350 m continues the upward coarsening progression displayed in the middle portion but becomes much coarser. The profundal lacustrine facies disappears and is replaced by deltaic or lake-margin deposits. Individual parasequences vary between deltaic or lake-margin and alluvial-fan and fan-delta conglomerates.

Since the initial establishment of the Zanda Formation as a lithological unit (*29*), additional formation (such as the Tuolin and Xiangze formations) or even group names (Zanda Group) were proposed (*30*), often based on a perceived depositional hiatus that later proved to be false (*31, 32*). Here we use a single unit name, Zanda Formation, for the entire basin sequence.

Magnetochronology and Biochronology. There have been no less than four independent attempts at paleomagnetic age determination of the Zanda strata during the past 11 years, although only three of these provided enough documentation to be evaluated here (*28, 32, 33*) (Zhu et al. (*30*) and Meng et al. (*34*) mentioned a paleomagnetic section of their own, but provided no detailed documentation). All three studies measured an 800+ m section for the total thickness of Zanda sediments, and arrived at roughly similar magnetic reversal patterns (not

surprisingly, sections with a higher density of sampling tend to detect more and shorter magnetochrons).

Qian's (*33*) first attempt used no independent age constraint and simply correlated his magnetic section (12 normal and 13 reversed magnetozones) to then "Chron 6" through Jaramillo Chron (6.15-1.5 Ma). Wang et al. (*32*) listed four fossil horizons in their more densely sampled magnetic section revealing 15 normal and 15 reversed magnetozones. Three of the horizons contain fossil mammals (*Hipparion zandaense*, *Ochotona* sp., and Dicerorhininae) and one with four species of gastropods. However, only one site yielded identifiable mammal (four cheek teeth of *Hipparion zandaense*), and the other two sites are inferred occurrences of *Ochotona* sp. (a single cheek tooth (*35*)) and a rhino (one metapodial (*34*)) collected from near the Dingdingka area, which is "40 km" north of Wang et al.'s (*32*) magnetic section according to Meng et al. (*34, 35*) (detailed locality information is not provided although this distance is probably greatly exaggerated). Furthermore, none of these fossils are well preserved or well studied enough to offer real constraints within their proposed age range of late Miocene through Pliocene.

Most recently, Saylor et al. (*31*) presented two more magnetic sections from the south and southeast Zanda Basin. A composite magnetic column was derived by combining each part of a section that has more magnetozones, and resulted in a total of 12 normal and 12 reversed zones. Saylor et al.'s south Zanda magnetic section was sampled from the same canyon as that by Wang et al. (*32*) (Zanda-Bolin section; see also Kempf et al. (*36*)), although individual measured segments (legs) differ from each other. It is thus reassuring that these two magnetic sections essentially replicate each other. Where Saylor et al. under-sampled at their 100-150 m level, Wang et al.'s much denser sampling revealed a relatively long reversed chron missed by Saylor

et al. (Fig. S3). For chronologic constraints, Saylor et al. (*31*) used past reports of vertebrate fossils (*Hipparion*, *Palaeotragus*, etc.) to constrain the Zanda strata to late Miocene through Pliocene and selected their preferred correlation by invoking a global C_3/C_4 vegetation transition at ~7 Ma.

A partial palate of a primitive giraffe, *Palaeotragus microdon*, was recovered near the Xiangze Farm area of the northern Zanda Basin during a preliminary survey of the Quaternary geomorphology by a Chinese Academy of Sciences expedition in 1976 (*29*). A nearly complete skull of a new hipparionine horse, *Hipparion zandaense* Li and Li, was described from exposures near the village of Daba in the southeastern Zanda Basin (*37*). Additional miscellaneous materials (isolated cheek tooth of *Ochotona* (*35*) and a rhino (Dicerorhininae) metapodial (*34*)) were collected from the Dingdingka area. The above isolated reports aside, there were no systematic efforts to collect fossil vertebrates prior to our field expeditions in 2006-07 and 2009-10. The holotype woolly rhino skull was collected from south of the main road entering Zanda Basin (Fig. S2) in the middle fine-grained sequence of the Zanda Formation.

Our own mammalian faunas offer, for the first time, the most restrictive age constraints so far known. Critically, in the lower part of the sequence, we have recovered a small mammal assemblage (IVPP localities ZD0609 and 0904) that falls in the 174-186 m level of Saylor et al.'s (*28, 31*) south Zanda section within the top part of an alternating greenish sandstone and silt unit and just below the fine-grained lacustrine mudstone with fine laminations. The most age-diagnostic element of this small mammal assemblage is *Mimomys*, represented by three upper first molars and one lower molar. In level of crown heights, our Tibetan material is most comparable to *Mimomys* (*Aratomys*) *bilikeensis* from the early Pliocene Bilike locality of Inner Mongolia, which is the earliest representative of arvicoline rodents in China (*38*). Arvicoline

rodents first appear in the early Pliocene of western Siberia (*39*) and shortly afterward dispersed to northern Asia (*38*), Europe (*40, 41*), and North America (*42-44*). The appearance of these rodents thus is a highly age-diagnostic event throughout northern continents. IVPP localities ZD0609 and 0904 fall in a relatively long normal chron that we interpret to be C3n.4n, i.e., 4.997-5.235 Ma in ATNTS2004 (*45*) (Fig. S3).

Large carnivorans, such as *Chasmaporthetes* (IVPP locality ZD0908), *Vulpes* (IVPP locality ZD1001), *Nyctereutes* (IVPP locality ZD0624), and *Meles* (IVPP locality ZD1001), offer additional chronologic constraints, even though most of these are stratigraphically 30 to more than 200 m higher than the *Mimomys* horizon. The Asiatic first occurrences of these genera are mostly confined to the Pliocene, although occasional late Miocene records have been suggested elsewhere (*46-49*). Collectively they have a distinctly Pliocene characteristic.

We would like to point out that a partial maxilla fragment with cheek teeth was described from the Xiangze section as *Palaeotragus microdon* (*29*). We were unable to find this primitive giraffe during our own collecting. However, we did collect a large cervid (left and right partial antlers, and isolated cheek teeth) from several localities (IVPP localities ZD0624, 1040, etc.), and we suspect that these belong to the same taxon (although we have not examined the original specimen described by Zhang et al. (*29*)).

Overall, the fossiliferous middle Zanda sequence yields characteristic Pliocene faunas (Table S1), although the upper alluvial conglomerates and lower fluvial sandstones, from which few vertebrate fossils are found thus far, range into the Pleistocene and Miocene, respectively. Based on our paleontologic constraints, we re-interpreted previously published paleomagnetic columns from various parts of the basin, and our new age estimates (Fig. S3) of the Zanda section spans ~400 Ka to 6.1 Ma in GPTS of ATNTS2004 (*45*). Our alternative interpretation is

closest (but not identical) to those proposed by Qian (*33*) and takes into account the fast

deposition in the upper conglomerates and lower fluvial sandstones.

Additional description and comparison of the woolly rhino (Figs. S4-S6; Tables S2-6).

Coelodonta thibetana has a skull length of 771 mm, close to the living white rhino

Ceratotherium simum (mean length = 797 mm), and much longer than the living Sumatran rhino

Dicerorhinus sumatrensis (mean length = 525 mm). The skull roof of the new species is concave

and bears broadly separated parietal crests (minimum distance 46.5 mm), as in other dicerorhines,

such as *Dihophus ringstroemi* (*50*) and *Stephanorhinus etruscus* (*51*). The relative size of the

nasal horn is greater than in extant and fossil rhinocerotines, and resembles those in elasmotheres

(*52-54*) or dicerotines (*55*) but narrower in shape. The morphology of the lower part of the nasal

septum in *Coelodonta thibetana* is not clear because the premaxilla is crushed. However, we can

observe that the nasal and premaxilla are separate by a distance of 74 mm between their tips.

This distance falls in the range of the basal dicerorhines (*55*) and extinct elasmotheres (*52*), and

it is longer than that of *C. nihowanensis* (*48*). In contrast, the nasal and premaxilla of the most

derived *C. antiquitatis* are in contact (*56*). The upper part of the septum is divided into two

branches, indicating that it was fused by two thin sheets of bone. The preserved portion of the

premaxilla is very narrow, indicating a reduced and edentulous premaxilla.

The nasals are very broad, as in other early *Coelodonta* (*57*), and their anterior ends bend

downward. The nasal notch is deep, with the posterior margin above the P3/P4 boundary. The

degree of nasal lengthening is similar to the state typically seen in Miocene to Pleistocene

dicerotines such as *Dihoplus ringstroemi* (*50, 58*) or *Stephanorhinus etruscus* (*51*), but less than

in forms with very elongated nasals such as *S. hundsheimensis* and *S. hemitoechus*, or in the

more derived species of *Coelodonta* (*57*). The nasals appear somewhat more lengthened and the notch correspondingly deeper than in *Coelodonta nihowanensis*. The nasal septum of *C. thibetana* is ossified along the anterior third of the nasal notch, similar to the degree of ossification in *S. hemitoechus* (*59*), but weak compared with more derived species of *Coelodonta* (*48, 57, 60*). The nasal septum has a distinct suture fused with the premaxilla, and its contact with the nasals is tight but not fused. The septum of the new woolly rhino is also relatively thin. The maximum anterior thickness is 36 mm, thinner than in *C. nihowanensis* (40 mm (*48*)) and *C. antiquitatis* (56 mm (*61*)).

The infraorbital foramen is open above the middle of P4, and the anterior border of the orbit is above the M2/M3 boundary. The lachrymal tubercle is strong, but the postorbital processes are absent on the frontal and zygomatic arch. The postglenoid process is long and strong, with a right dihedron in cross section, and it is fused with the posttympanic process to form a closed external auditory pseudomeatus.

In the atlas, the outline of the rachidian canal is mushroom-like; the fovea dentis is shallow; the alar fossa is present; the inferior alar foramen is very small; the lateral vertebral foramen is absent, which is present in *C. antiquitatis* (*56*). The axis is short, with a high spinous process whose cranial border is sharp; the cranial intervertebral notch is broad, but it tends to close and form an intervertebral foramen as in *C. antiquitatis* (*56*). The third cervical vertebra is relatively short and high, without the mammillary process, which is strongly developed as in *C. antiquitatis* (*56*) (Fig. S6).

The mandible is nearly complete. The lower incisors are absent, but there is a small alveolus on the left jaw, indicating the presence of a deciduous second incisor, as also seen in *C. nihowanensis* (*48*). In lateral view, the symphysis is elevated and forwardly positioned, which is

similar to that of *C. nihowanensis* (*48*). The lower border of the horizontal ramus is straight behind the level of m1. The posterior border of the mandibular symphysis is in front of the p2, more anterior than that of the Quaternary woolly rhinos (*48, 56*). The mandibular angle is rounded, and the ascending ramus is reclined posteriorly. *Stephanorhinus etruscus*, another known Pliocene dicerorhine with well-preserved mandible, differs from *C. thibetana* in possessing a more backward posterior symphysis reaching the p2/p3 boundary and a more vertical ascending rami (*51*). The backward shift of the mandibular symphysis is an evolutionary trend among species of *Coelodonta* (*62*). The posterior border of the symphysis in *C. nihowanensis* is situated at the p2/p3 boundary (*48*), whereas it is at the middle of p3 in the derived Eurasian species *C. antiquitatis* (*55*). The symphysis of *C. thibetana* is much more forward in comparison with those of *C. nihowanensis* and *C. antiquitatis*, representing a more primitive condition within the genus.

Dental morphology of *C. thibetana* falls well within the diagnosis of the genus (*48*). The P1 and p1 are absent. The crown is high, with a weak cement cover on the labial wall. The median valley is closed on the premolars. The crochet and crista are well developed, and the medi- and post-fossettes are visible at an early stage of wear, which are different from those of *Stephanorhinus*, which lacks the medi- and post-fossettes (*51*). The upper teeth are similar to those of *C. nihowanensis* (*63*), and minor differences between the two species mainly lie in the molars: the ectoloph is weakly wavy, the M1 lacks the crista, and the M2 has a less well-developed mesostyle in *C. thibetana*. The upper teeth of *C. antiquitatis* are markedly different from those of *C. thibetana* and *C. nihowanensis* in having the strongly wavy labial wall, thick cement cover, a strongly backwardly slanting protocone, and a quadrate outline in the M3 (*55, 56*).

The p2 has an elongate triangular outline with a paraconid, but the left p2 is absent

abnormally. The differences in the p3–m3 among *C. nihowanensis*, *C. tologoijensis*, *C.*

antiquitatis, and *C. thibetana* are remarkable. *C. tologoijensis* and *C. antiquitatis* are more

derived than the other two species in having a posterior edge of the protoconid, and swollen

metaconid and entoconid (*56, 64*). *C. nihowanensis* has strong anterior and posterior ribs on the

labial wall of the trigonid (*48*), but *C. thibetana* possesses blunt anterior and posterior external

corners on the lower teeth, and a weak anterior rib on m2-3.

Phylogenetic Analysis. To evaluate the phylogenetic position of *Coelodonta thibetana*

within Rhinocerotinae, a phylogenetic analysis of 17 well-known rhinocerotid taxa was

performed. The following taxa formed the ingroup: *Lartetotherium*, *Ceratotherium simum*,

Diceros bicornis, *Dicerorhinus sumatrensis*, *Rhinoceros sondaicus*, *Rhinoceros unicornis*,

Stephanorhinus etruscus, *Stephanorhinus hundsheimensis*, *Stephanorhinus hemitoechus*,

"Dihoplus" kirchbergensis, *Dihoplus megarhinus*, *Dihoplus pikermiensis*, *Dihoplus ringstroemi*,

Coelodonta nihowanensis, *Coelodonta tologoijensis*, *Coelodonta antiquitatis*, and *Coelodonta*

thibetana (this study). *Ronzotherium* acted as an outgroup. The 46 characters used in this study

were mainly taken from a previous analysis by Antoine (*62*) but several characters were modified

and seven new characters were added (for a complete list of characters and the character matrix

see Tables S7 and S8). Character states were scored according to published literature and

personal records of museum specimens. The data set was analyzed using the branch-and-bound

algorithm with ACCTRAN optimization in PAUP* 4.0b10 (*65*). Characters were left un-

weighted and un-ordered. 'Gap' states were treated as 'missing data'. Bootstrap analysis (1000

replicates) was also performed using PAUP* 4.0b10, and decay analysis was performed using

PAUP* 4.0b10 and TreeRot 2.0 (*66*).

The branch-and-bound search found nine most parsimonious trees (tree length = 139, consistency index = 0.439, retention index = 0.569, homoplasy index = 0.561, rescaled consistency index = 0.250). The nine most parsimonious trees (MPTs), together with a strict consensus (with decay and bootstrap values shown) and 50% majority consensus of these trees, are shown in the supporting figures (Figs. S7-S9).

As can be seen in the strict consensus tree (Fig. S8), only two of the grouping found in all of the trees received over 50% bootstrap support (50% for the *C. simum – D. bicornis* clade and 67% for the *C. tologoijensis – C. antiquitatis* clade), which reflects a high degree of homoplasy within the different branches. However, most clades, including the *Coelodonta-Stephanorhinus-Dihoplus* clade and the *Coelodonta* clade, received relatively good support from the decay analysis (decay value of 3). Only two clades received a decay value of 1. Both of these are for groupings within the *Stephanorhinus-Dihoplus* clade, revealing that the interrelationships between these species will change in trees with just one step longer.

For the extant rhinos (*Ceratotherium simum*, *Diceros bicornis*, *Dicerorhinus sumatrensis*, *Rhinoceros sondaicus*, *Rhinoceros unicornis*), the results of our analysis (Figs. S7-S9) are in agreement with the recent analysis by Tougard et al. (*67*) and Willerslev et al. (*68*), which were based on mitochondrial genome sequences, and with the morphological analysis by Antoine (*62*), which was the source of most of our characters. However, the position we recovered for *Coelodonta* in relation to the extant taxa is different from its position in Antoine (*62*) and Willerslev et al. (*68*) (no fossil taxa were included in Tougard et al.'s (*67*) analysis). We found that *Dicerorhinus sumatrensis* either formed a sister group with the two *Rhinoceros* species, and this clade was the sister group of the *Coelodonta-Stephanorhinus-Dihoplus* clade (Fig. S7d-f), or

the two *Rhinoceros* species formed the sister group of the *Coelodonta-Stephanorhinus-Dihoplus* clade, while *Dicerorhinus sumatrensis* was the sister taxon of this larger grouping (Fig. S7a-c, g-i). In contrast, Antoine (*62*) recovered *Coelodonta antiquitatis* as the sister taxon of the *Diceros-Ceratotherium* clade, whereas in Willerslev et al. (*68*) *Dicerorhinus sumatrensis* was the sister taxon of *Coelodonta antiquitatis*. However, in both of these analyses *Coelodonta antiquitatis* was the only extinct rhinocerotine taxon included. Thus, increasing the number of extinct rhinocerotine taxa appears to have an impact on the resulting relationships between *Coelodonta* and the extant rhinos in a morphological phylogenic study. It is very likely that if molecular data of more numerous fossil taxa were added into the analysis of Willerslev et al. (*68*), the results of that study would also change, especially as the interrelationships between the extant rhino clades were not conclusively resolved. Of other (fairly) recent analyses, Groves (*69*), Prothero et al. (*70*), and Cerdeño (*71*) have included both *Coelodonta* and *Stephanorhinus*. In accordance with our results, they found them to be sister taxa, although in the trees of Groves (*69*) and Prothero et al. (*70*) the sister group of the *Coelodonta-Stephanorhinus* clade was *Rhinoceros* (together with *Gaindatherium* and *Punjabitherium*, which were not included in this analysis), and in the tree by Cerdeño (*71*) the sister group was the *Elasmotherium-Ningxiatherium* clade. We did not include any elasmotheres in our analysis because they are clearly a monophyletic group characterized by a strong suite of autapomorphies, and are evolutionary distant from *Coelodonta* and *Stephanorhinus* (*62, 72*).

The locomotory skeleton of *C. thibetana* is unknown, but all other woolly rhinos except the terminal *C. antiquitatis* were cursorial forms. One of the most interesting questions left open by the new discovery is whether cursoriality was the original condition of this genus. It is conceivable that the high-altitude *C. thibetana* might have been short-legged, and that the

phylogeny of *Coelodonta* will turn out to be more complicated than the simple transformation series that our present analysis suggests. A rather stocky rhinoceros metapodial from Zanda (*34*) might be taken as support for such a scenario although this specimen has no associated cranial or dental materials. The derived character of stronger nasal lengthening and stronger inclination of the occiput seen in *C. thibetana* compared with the younger *C. nihowanensis* might also reflect such previously unrecognized complexity.

Additional paleoecologic considerations. Based on their high crowned cheek teeth with cement, long nasal horn, nasal septum, backward slanting occiput, dicerorhines, except phylogenetically enigmatic *Dicerorhinus*, were reconstructed as grazers (*15*, *73*, *74*). Relatively broad nasals with an ossified septum indicate that *C. thibetana* has two large nasal cavities for increased heat exchange in frigid air. The body weight of *C. thibetana*, estimated from its skull length, is about 1800 kg (*75*). The body size of an endothermic mammal is important in determining its metabolic requirements. The maintenance requirements of per unit body weight decrease with increasing body weight. Among herbivores this means that absolute body size is very important in determining the fibre/protein intake ratio that an animal will be able to tolerate in its diet, as larger mammals require proportionally less protein and thus are able to tolerate a larger proportion of cellulose (*76*). The Zanda woolly rhino is about the same size as *C. nihowanensis* but is smaller than *C. antiquitatis*, which achieved a larger body size during the colder late Pleistocene (Tables S2-S3).

The molars, while close to the plesiomorphic primitive type seen in related genera such as *Stephanorhinus*, already show signs of the modifications that become so striking in the late Pleistocene *C. antiquitatis*, a true grazer (*57*). The increased molar crown height, the presence of

coronal cement, and the incipient thickening of the enamel lining of the fossettes are all indicators of a shift towards a more abrasive diet (*77*). The cusp tips of the upper molars are worn to a distinctly rounded shape, neither sharp as in browsing rhinoceroses nor blunt as in true grazers, also indicating a mixed diet with a significant component of grass (*78*). The morphology and occlusal wear of the cheek teeth thus suggests that *C. thibetana* was a mixed feeder with a tendency to graze, like *C. nihowanensis* and *C. tologoijensis* (*57*).

The ability to sweep snow with a large, forward-leaning nasal horn may have been the most critical adaptation for surviving the harsh Tibetan winters, and as such, represents a unique evolutionary advancement for the woolly rhino lineage. Such a simple yet vital innovation, formed prior to the initiation of a permanent northern ice sheet, was a key pre-adaptation that opened the path to success for the woolly rhino in the mammoth fauna during the late Pleistocene.

Paleodiets and paleoenvironment. Carbon and oxygen isotopic compositions of fossil tooth enamel and bones contain valuable information about the diet and water composition, and paleotemperature (*79-82*). Specifically, $\delta^{13}C$ of tooth enamel from herbivores reflects the proportion of C_3 and C_4 plants in their diet. C_3 plants, which include all trees, cool season grasses and most shrubs, have $\delta^{13}C$ values ranging from -20‰ to -35‰, with a mean of -27‰ (*79, 83*). Under water-stressed conditions and/or low atmospheric partial pressure of CO_2 (*p*CO_2), C_3 plants are enriched in ^{13}C and have $\delta^{13}C$ values higher than the average value of –27‰. Under closed canopies, C_3 plants have lower $\delta^{13}C$ values (<-27‰) due to the influence of soil respiration (e.g., *79*). C_4 plants are mostly warm climate grasses and have $\delta^{13}C$ values of -9‰ to -17‰, averaging -13‰ (*79, 83*). Because tooth enamel from herbivores is consistently enriched in ^{13}C by ~14‰ relative to the diet due to biochemical fractionation, animals that eat C_3

vegetation typically have $\delta^{13}C$ values less than -9‰; animals that eat C_4 plants have $\delta^{13}C$ values >-2‰; and mixed feeders that eat both fall somewhere in between these two extremes (e.g., *79*). In much of the modern Himalayan-Tibetan Plateau, which is characterized by severe water-stressed conditions and low atmospheric partial pressure of CO_2 (*p*CO_2), the conservative "cut-off" enamel-$\delta^{13}C$ value for a pure C_3 diet should be -8‰ (*81*). We analyzed the carbon and oxygen isotopic compositions of 110 serial and bulk enamel samples from 25 teeth or tooth fragments from a diverse group of middle Pliocene mammals (including horse, rhino, deer, and bovid) and 60 bulk and serial enamel samples from nine teeth from eight modern Tibetan wild asses (*Equus kiang*) from Zanda Basin.

The average $\delta^{13}C$ value of enamel samples from modern wild Tibetan asses from Zanda Basin is -8.8±1.7‰, indicating a C_3-based diet and consistent with the current dominance of C_3 vegetation in the area. The enamel-$\delta^{13}C$ values for the time period of 3.1–4.0 Ma are -9.6±0.8‰ (n=110), indicating that these ancient herbivores fed primarily on C_3 vegetation and lived in an environment dominated by C_3 plants (Fig. 2B). Carbon isotope analysis of fossil plant materials in the basin showed that C_4 grasses were present in local ecosystems in the latest Miocene and Pliocene (*31*). Our enamel $\delta^{13}C$ data, however, suggest that C_4 grasses must have been a minor component of local ecosystems at ~3.1-4.0 Ma because they were insignificant in herbivores' diets (Fig. 2B).

The enamel- $\delta^{18}O$ values from modern wild Tibetan asses range from -7.4‰ to -12.8‰, averaging -8.8±2.1‰ (n=9). Enamel samples from the mid-Pliocene herbivores yielded $\delta^{18}O$ values ranging from -10.6‰ to -18.9‰. Studies have shown that the $\delta^{18}O$ of tooth enamel from an obligate drinker (such as horse and rhino) tracks the $\delta^{18}O$ of local meteoric water (*81, 84, 85*). Using the enamel-water $\delta^{18}O$ relationship for obligate drinkers (*84*), we estimated the $\delta^{18}O$

values of modern- and paleo-water from the δ^{18}O values of enamel from horse and rhino found in the Zanda Basin (Fig. 2C). The uncertainty in the water δ^{18}O estimates corresponds to 1 sigma (1σ) standard deviation in δ^{18}O of enamel. The estimated modern water-δ^{18}O values are -11.0$\pm$2.1‰, which are within the measured δ^{18}O values of modern stream waters (ranging from -7.3‰ to -17.9‰) in the Zhada Basin (*31*). The estimated δ^{18}O values of paleo-water in the mid-Pliocene is -13.9$\pm$0.6‰ at ~4 Ma, -19.4$\pm$1.0 at ~3.8 Ma, and -18.5$\pm$0.9‰ at ~3.5 Ma, which are lower than the estimated modern water δ^{18}O value based on enamel- δ^{18}O of wild Tibetan asses (Fig. 2). This positive δ^{18}O excursion likely indicates a shift to more arid conditions in the basin after the mid-Pliocene (Fig. 2).

Mammals Endemic to Tibetan Plateau and Megafauna Origins. Despite the rich Pliocene rhinoceros record of the Old World, no definitive pre-Pleistocene finds of *Coelodonta* have previously been reported; for example, none of the 173 Old World Pliocene rhinocerotid-bearing localities in the NOW database (*86*) include this genus (Fig. S10).

At present, the Tibetan Plateau is characterized by a high-altitude, low diversity, cold-adapted mammal fauna with over half of its species being endemic to the region due to high barriers of surrounding mountains (such as the Himalayas) and harsh environment in the high plateau (*87, 88*). Common extant large mammals in high Tibet include Tibetan wild yak (*Bos mutus*), Tibetan wild ass (*Equus kiang*), argali (*Ovis ammon*), bharal or blue sheep (*Pseudois nayaur*), chiru or Tibetan antelope (*Pantholops hodgsonii*), Tibetan gazelle (*Procapra picticaudata*), white-lipped deer (*Cervus albirostris*), lynx (*Lynx lynx*), snow leopard (*Panthera (Uncia) uncia*), etc. Of these, six have some fossil records or molecular evidence to suggest a Tibetan origin and we briefly treat them in the following paragraphs.

The Tibetan wild yak, *Bos mutus*, is the most charismatic and representative of Tibetan large mammals, and with its large body size and woolly rhino-like long, shaggy hair, may be the closest to the woolly rhino in its special adaptations to the cold open habitats. Although fossil yaks are extremely rare so far, it may have a Pleistocene distribution as far north as the Lake Baikal region in southern Russia (*89, 90*) and the Holocene of northern Pakistan (*91*). Recent molecular evidence consistently placed the Tibetan yak and European/American bison as a sister group (*92-95*), as did a supertree attempt (*96*), and most seem to agree that yak and bison arose from a common ancestor in central Asia, whereas the American bison crossed the Bering Land Bridge to invade the New World in the late Pleistocene (*97, 98*). Thus, the case for the cold-adapted yak to give rise to the Pleistocene bison in the northern Holarctic deserves further investigation.

The case for the argali, *Ovis ammon*, bears distinct similarities to the yak in its relationship to North American megafauna. The argali is the basal stock to give rise to the North American Dall's sheep (*Ovis dalli*) and bighorn (*Ovis canadensis*), through a transitional snow sheep (*Ovis nivicola*) of eastern Siberia (*99, 100*). These sheep arrived at North America as the last wave of immigrants during the Rancholabrean land mammal age (*43*). As in the case of above *Bison-Bos mutus* sister relationship, the preference to cold and mountainous habitats by *Ovis* seems a striking link between argali, snow sheep, and bighorn. The argali has a present distribution in the Tibetan Plateau and surrounding mountains to the north and west, and its Pleistocene distribution is much greater (*101*), possibly as far west as France (*102*), as would be expected for a cold-loving species during the Ice Age. Unfortunately, there are no Tibetan records for fossil *Ovis*, even though sheep horncores tend to be well-preserved.

A similar connection was made between the Tibetan ass, *Equus kiang*, and fossil horses in the late Pleistocene of Alaska (*103, 104*), although such a hypothesis has been questioned (*105*). Morphological similarity between *Equus kiang* and the extinct *E. sivalensis* from the Pleistocene of India and Pakistan has been noted (*106*), although the exact locality and age for the latter's holotype remain ambiguous (*107*). It seems premature to draw firm conclusions from these studies, but it is conceivable that the center of evolution of the ass group could be related to the Siwalik form (*108*).

The somewhat goat-like Tibetan bharal (or Blue Sheep), *Pseudois*, is presently endemic to the Tibetan Plateau, preferring mountainous terrains above the tree line between 4,000-6,000 m in elevation (*109, 110*). Previous records of the bharal are known in the middle to late Pleistocene of north China (*111-113*), reaching as far as Liaoning Province in Northeast China, more than 1,800 km northeast of the Tibetan Plateau. However, its Pleistocene record appears to be confined to mountainous areas or in caves. Such a preference to rocky terrains may be the main reason that the bharal did not expand as far north as the woolly rhino. A nearly complete left and right horncore of possibly an ancestral species of *Pseudois* was found in IVPP locality ZD0712 in Zanda Basin, 1.57 km northeast of the type locality of the new woolly rhino and stratigraphically approximately 30 m above. Distantly related to the goat rather than sheep (*114, 115*), the Bharal possesses a mixture of morphologic characters of both (*109*). The Zanda form, with its laterally divergent horncores, semi-rounded (with a slight hint of triangular) cross-sections, and relatively smooth surface, is closest to *Pseudois* among extant Tibetan bovids (*109*) (Fig. S11). Its horncore orientation, however, still has a significant caudal component, as contrasted to an essentially lateral orientation in modern and Pleistocene forms (*112*), suggesting a more primitive condition for the Pliocene Tibetan form. If this horncore does belong to

Pseudois, or a more primitive relative of it, then the bharal is another example of a Tibetan ancestor giving rise to Pleistocene megafauna.

The origin of the chiru (Tibetan antelope), *Pantholops hodgsonii*, offers another interesting case of a Tibetan endemic species, whose ancestry can be traced as far back as the late Miocene. In Qaidam Basin in the northern Tibetan Plateau, *Qurliqnoria*, an extinct bovid with a straight, upwardly oriented horncore, has been regarded as ancestral to the chiru (*116*). A horncore fragment of *Qurliqnoria* was found in the early Pliocene strata (IVPP locality ZD0745, ~4.2 Ma) of the Zanda Basin (Fig. S12). Intriguingly, late Miocene mammals from Qaidam Basin began to show a modest level of endemism in the Tuosu and Shengou faunas (*117*). Peculiar bovids, such as *Tsaidamotherium*, *Olonbulukia*, *Qurliqnoria*, *Tossunnoria*, and species of dicrocerine deer (unpublished materials possibly referable to *Euprox*), are almost exclusively restricted to the Qaidam region. An extinct Pleistocene species of the chiru, *Pantholops hundesiensis*, was described from the high elevation "Hundes plain" near the present day Niti Pass of India (*118*). An undescribed horncore of *Qurliqnoria/Pantholops* from the Plio-Pleistocene Kunlun Pass Basin (elevation 4,700-5,000 m) in north-central Tibet (*119, 120*) also hints at its long history in the plateau. Assuming *Qurliqnoria* is closely related to *Pantholops*, as horncore morphology seems to suggest, then the case for a Tibetan origin of the chiru is strongly indicated.

The snow leopard, *Panthera* (*Uncia*) *uncia*, is another endemic Tibetan species. Although questionable Pleistocene records from Europe and Asia have been referred to the snow leopard (*121-124*), most of which has been refuted (*125-127*), a more credible reference is from a more recent discovery in an early Pleistocene locality in the "upper Siwalik" of Pabbi Hills in northern Pakistan (*128, 129*). We were very fortunate to have recovered cranial and dental

material of an ancestral snow leopard from IVPP locality ZD1001 in Zanda Basin in 2010 (Fig. S13). Its skull possesses a compressed frontonasal region and an expanded maxillary above the infraorbital foramen, features that are characteristic of the snow leopard (*130*). ZD1001 is early Pliocene (~4.4 Ma) in age, and this new snow leopard is undoubtedly the earliest record of its kind, offering another unambiguous record of the megafauna origin in Tibet.

To sum up, of the eight endemic modern Tibetan or otherwise high altitude, cold-adapted large mammals (*Bos mutus*, *Equus kiang*, *Ovis ammon*, *Pseudois nayaur*, *Pantholops hodgsoni*, *Procapra picticaudata*, *Cervus albirostris*, *Panthera* (*Uncia*) *uncia*), fossil occurrences for three (*Pseudois nayaur*, *Pantholops hodgsonii*, *Panthera* (*Uncia*) *uncia*) can be traced to an earlier ancestry in Tibet in the late Miocene or early Pliocene. Three other large ungulates, *Bos mutus*, *Equus kiang*, and *Ovis ammon*, offer strong molecular or circumstantial fossil evidence for a Tibetan ancestral stock to give rise to forms that were able to expand to the mammoth "steppes" in northern Eurasia during the late Pleistocene, and in the case of *Bison* (sister of *Bos mutus*) and *Ovis*, were able to cross the Bering Land Bridge to settle in North America. Therefore, at least for some high latitude Holarctic megafauna components, a Tibetan origin should be seriously entertained.

Given the low diversity of modern Tibetan mammal fauna, a high percentage of them either have a long residential history in the plateau going back to at least Pliocene, suggesting long periods of habituation within the confines of the high plateau, or expanded their range during the Pleistocene to become significant players in the high latitude Holarctic megafauna. With its formidable cold climate and thin air, the Tibetan Plateau may thus have served as a habituation ground during the Pliocene, and as arctic and boreal habitats expanded during the Ice

Age, the Tibetan megafauna found itself in an advantageous position to conquer the rest of northern Eurasia and even of North America.
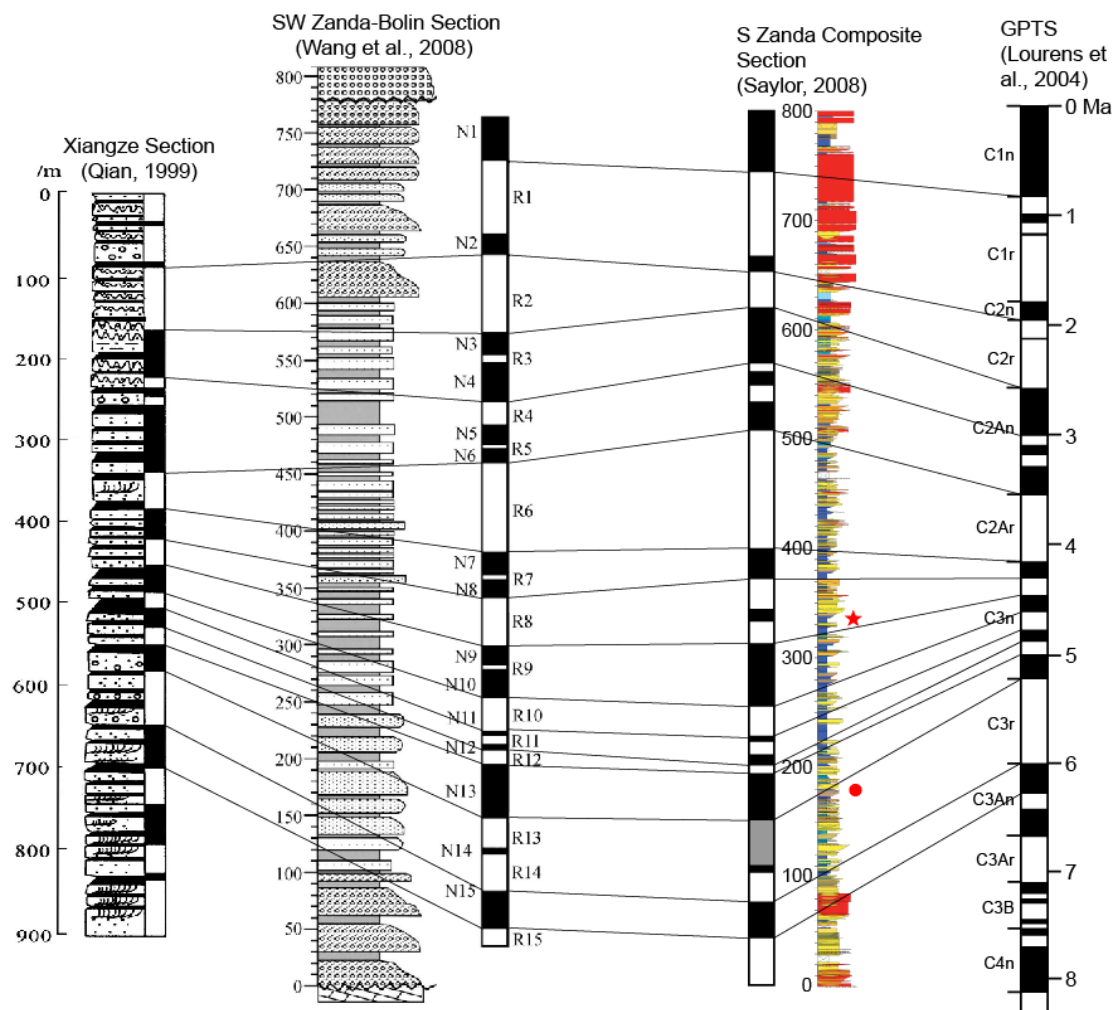
Figures in Supporting Online Material
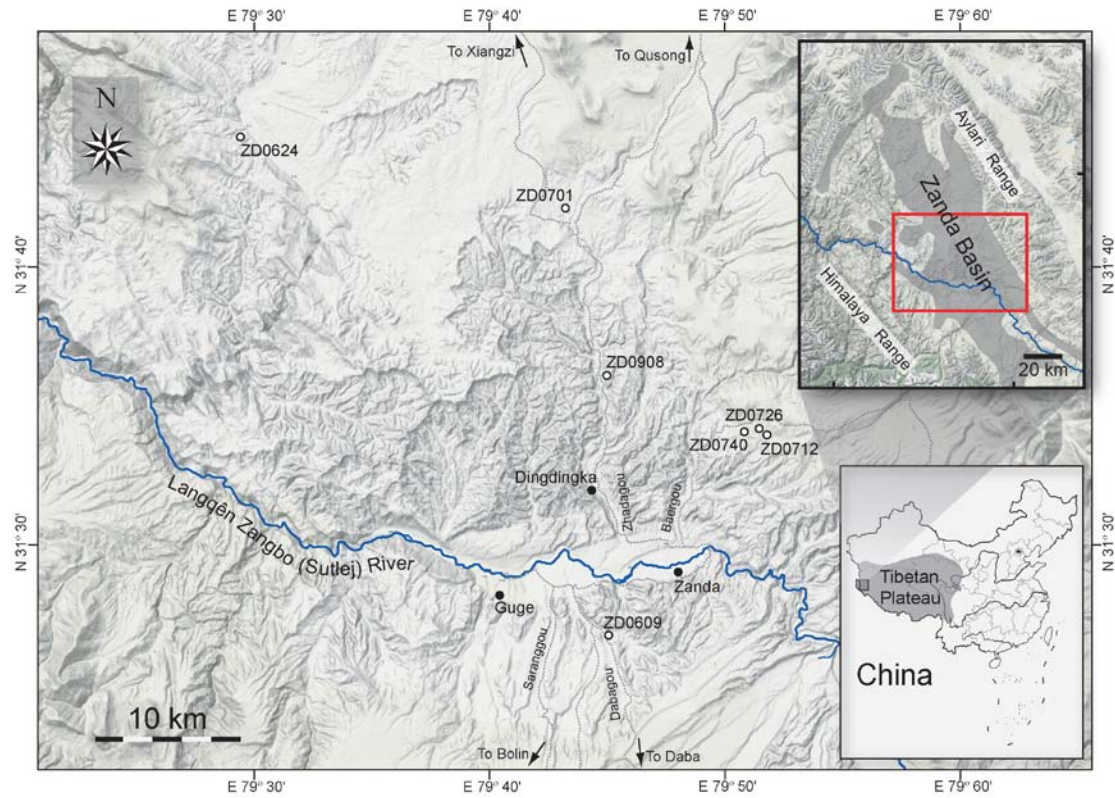
Fig. S1. Map showing important fossil localities and important geographic locations discussed in the text. Map source: Google Earth.

Fig. S2. Exposures of fluviolacustrine sediments where the holotype of *Coelodonta thibetana* sp. nov. (IVPP V15908) was found (red arrow), Zanda Basin, Ngari District, Tibet Autonomous Region, China.

Fig. S3. Correlation of three published paleomagnetic sections and stratigraphic positions of key Zanda fossil mammal localities. Vertebrate fossils are placed in the nearest measured sections by Saylor (*28*), which are in turn correlated on the basis of intrabasin sequence stratigraphic criteria. Red star indicate woolly rhino locality (ZD0740) and red circle indicate key fossil sites (ZD0609, 0904) for biochronologic constraints. Ages for magnetic chrons in the Geomagnetic Polarity Time Scale (GPTS) are based on ATNTS2004 in Lourens et al. (*45*).

Fig. S4. Holotype of *Coelodonta thibetana* sp. nov. (IVPP V15908). Ventrolateral view of the skull.
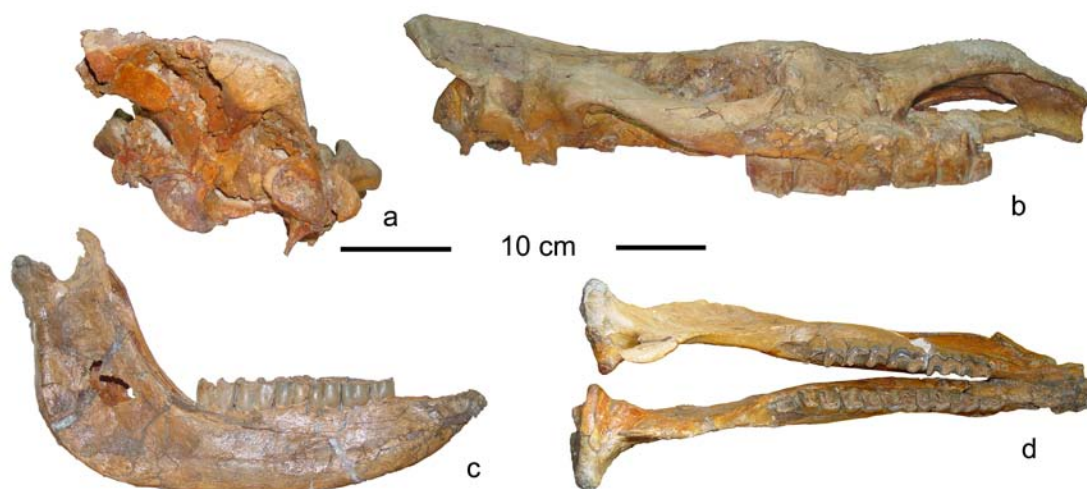
Fig. S5. Holotype of *Coelodonta thibetana* sp. nov. (IVPP V15908). (**a**) Occipital view of the skull; (**b**) lateral view of the skull; (**c**) lateral view of the mandible; (**d**) occlusal view of the mandible. Scale bars, 10 cm, left for a, and right for b, c and d.
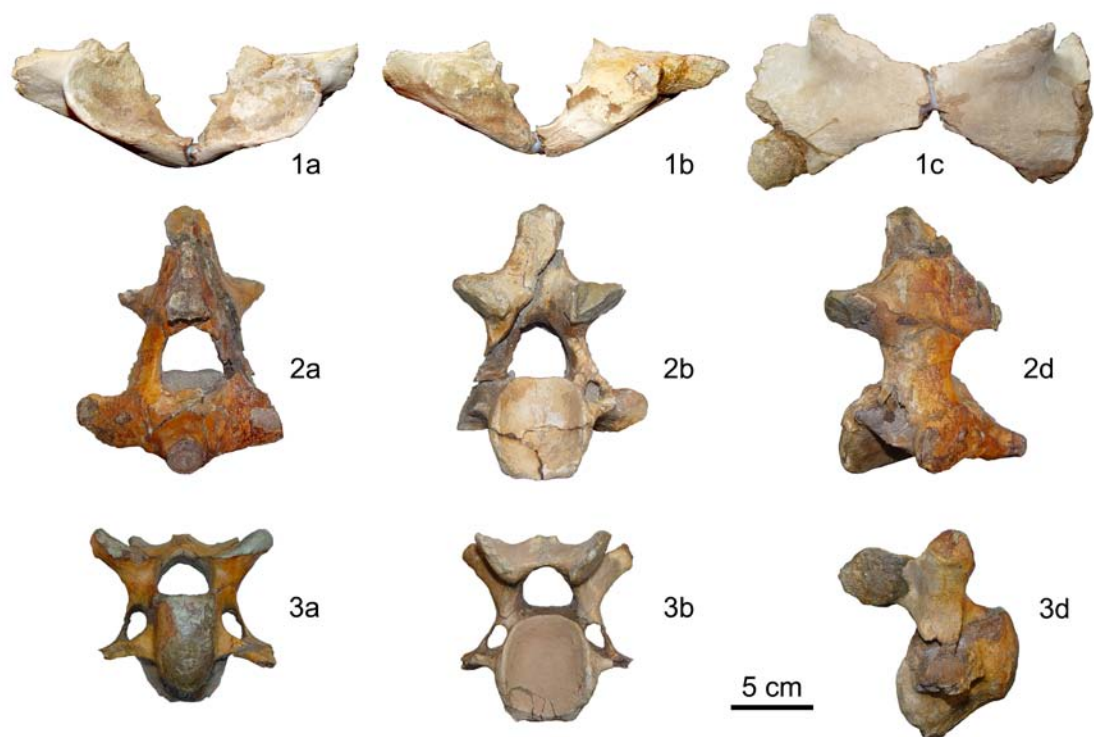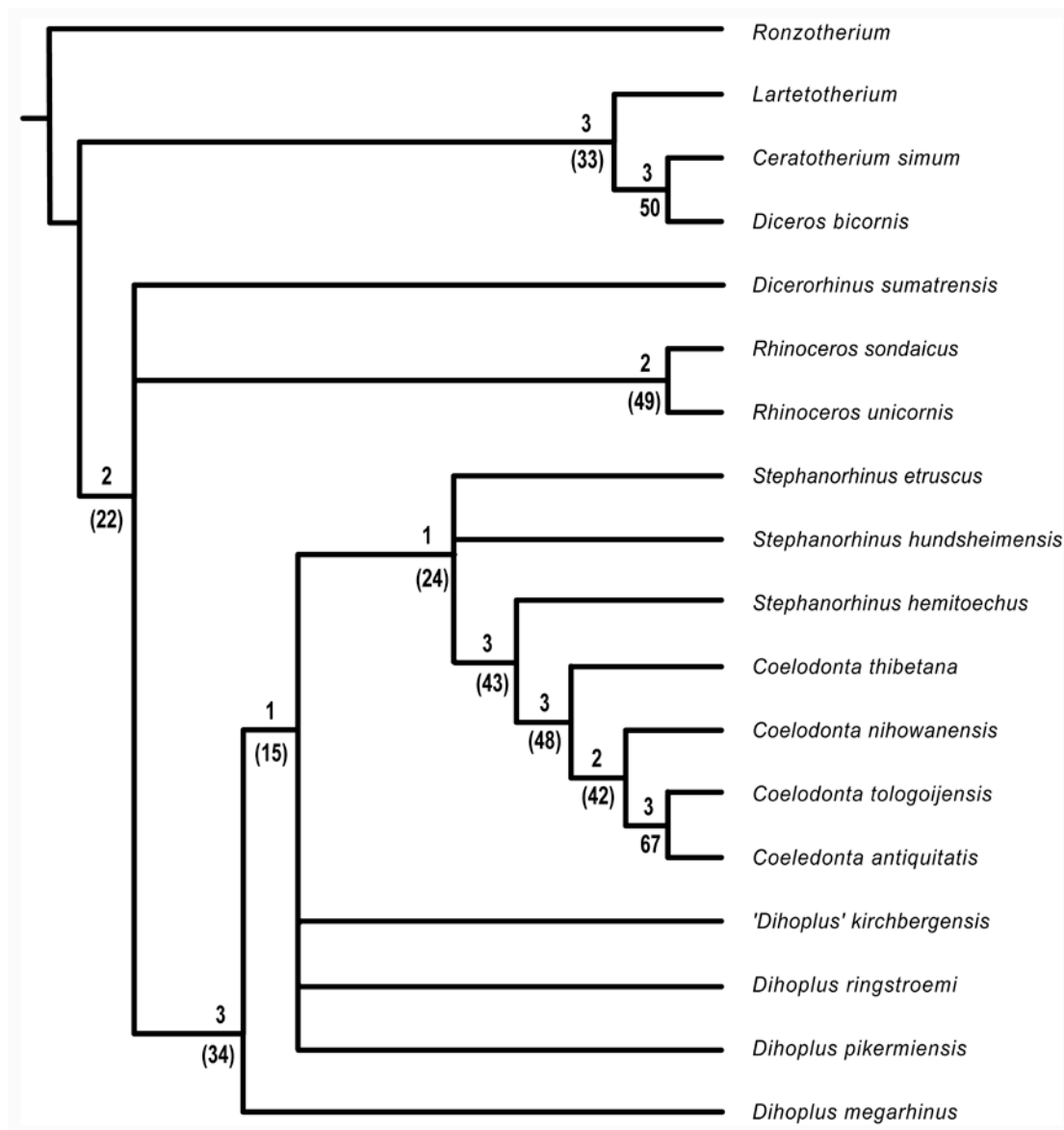
Fig. S6. Holotype of *Coelodonta thibetana* sp. nov. (IVPP V15908). (**1**) atlas; (**2**) axis; (**3**) third cervical vertebra. (**a**) cranial, (**b**) caudal, (**c**) ventral, and (**d**) lateral view.
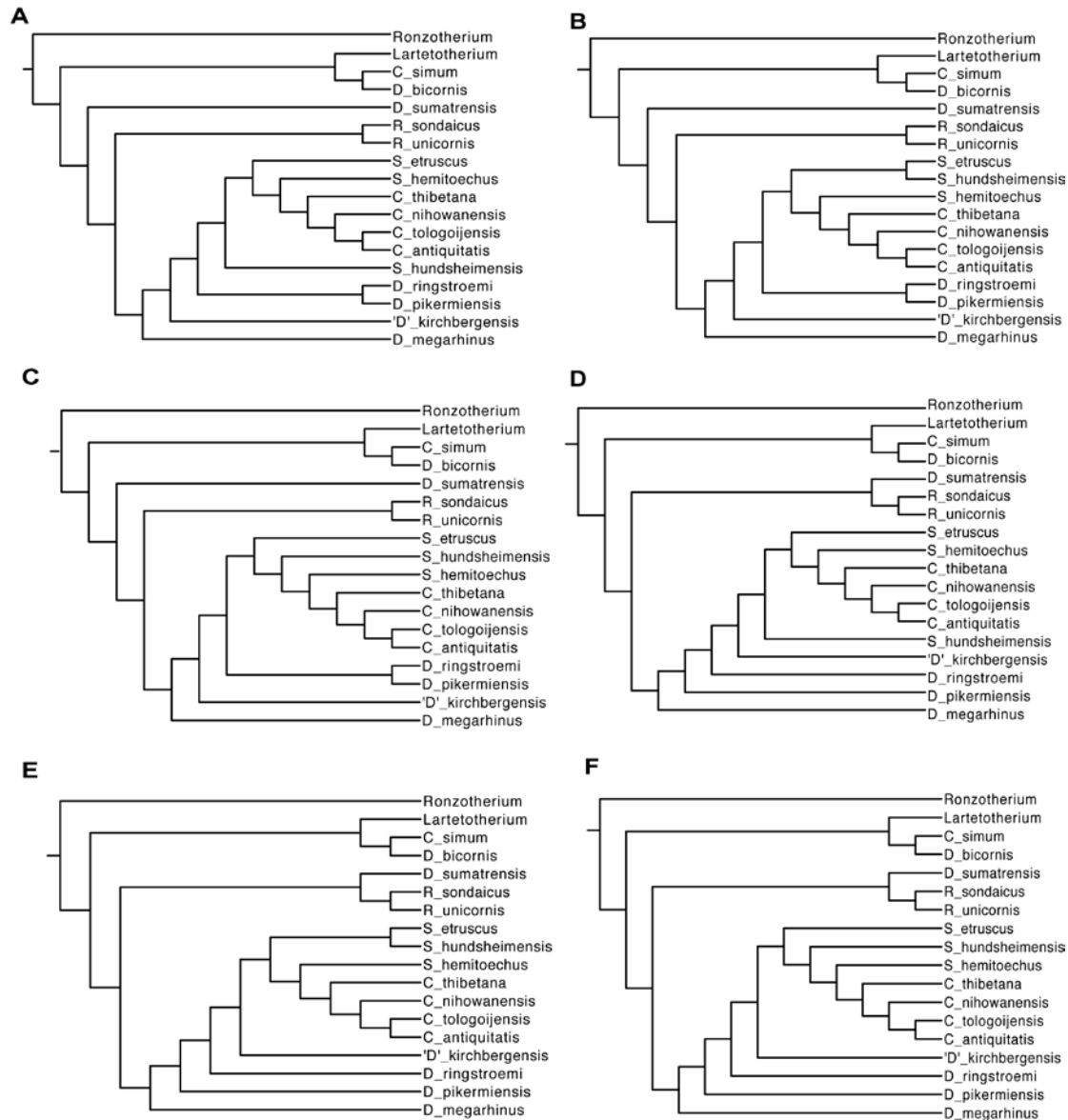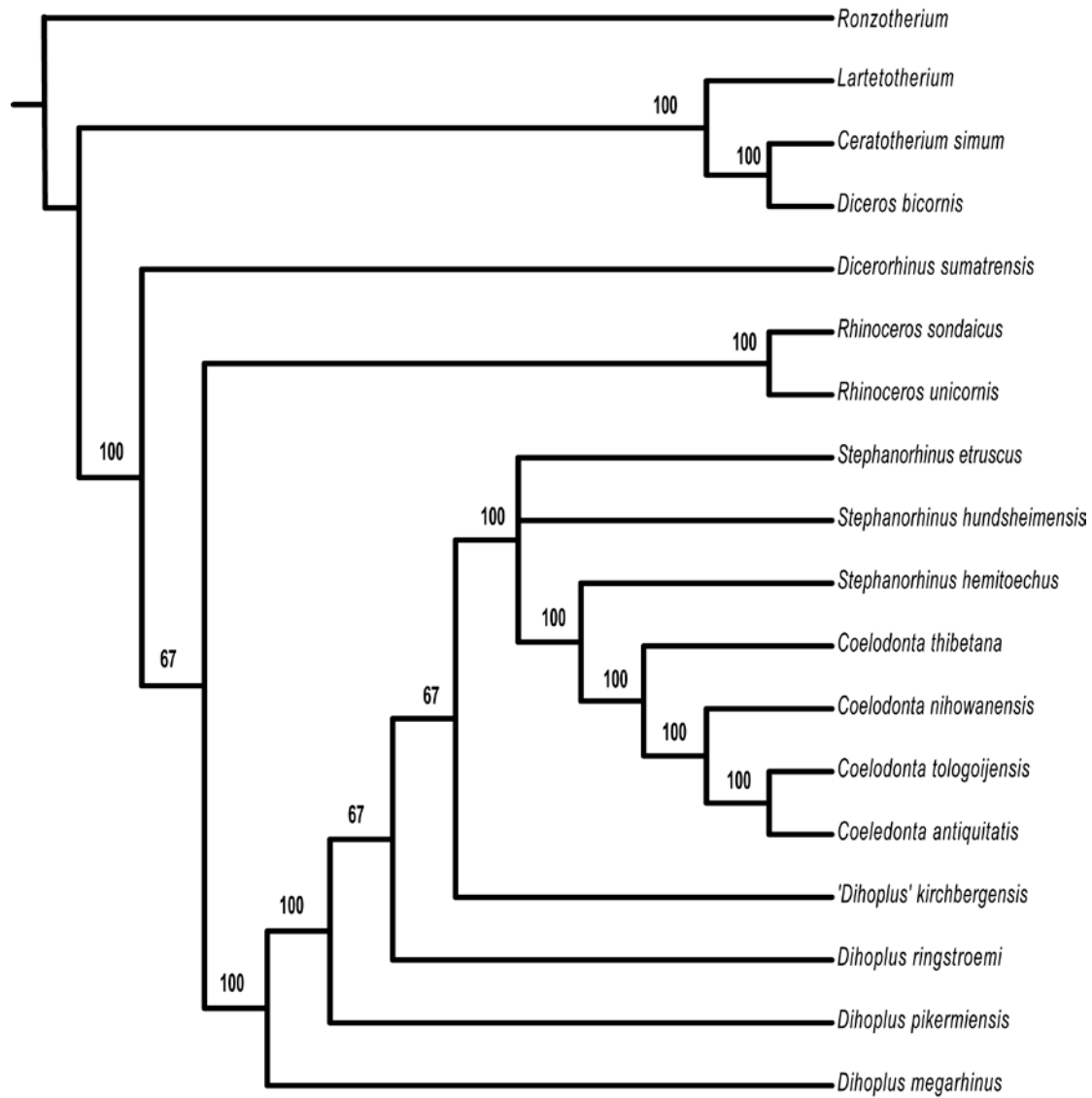
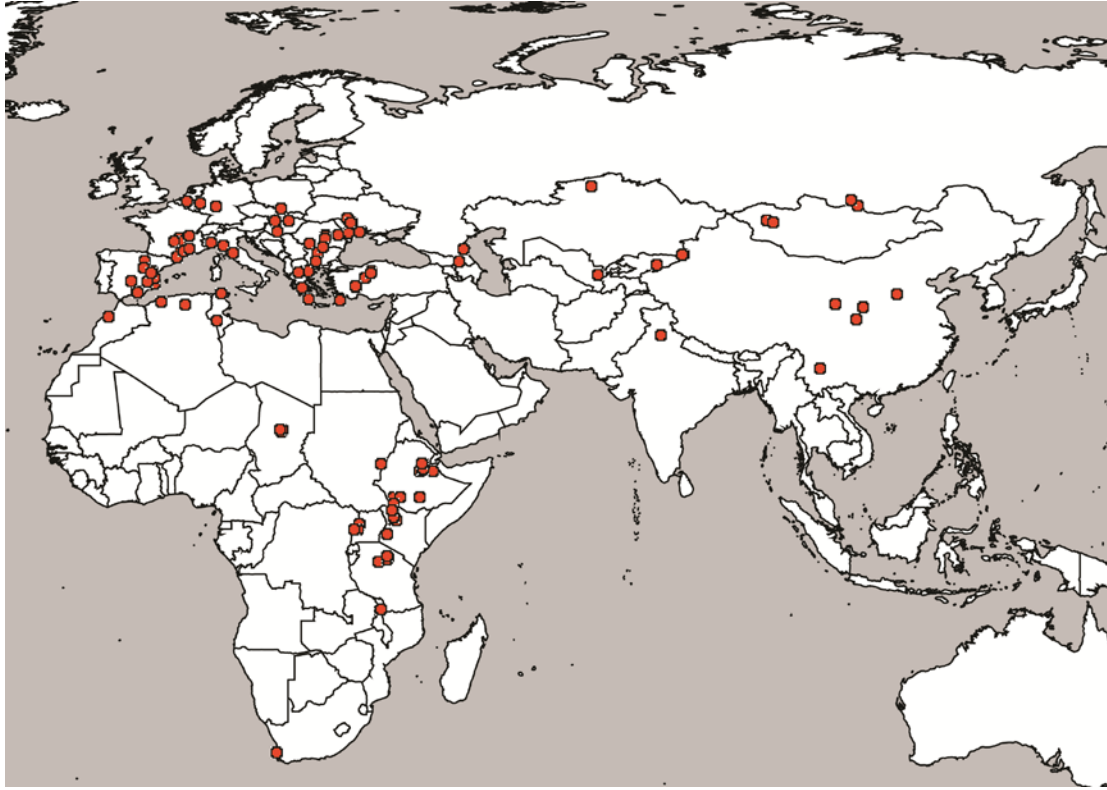**Fig. S7**. Nine most parsimonious trees of the phylogenetic analysis of Rhinocerotini.
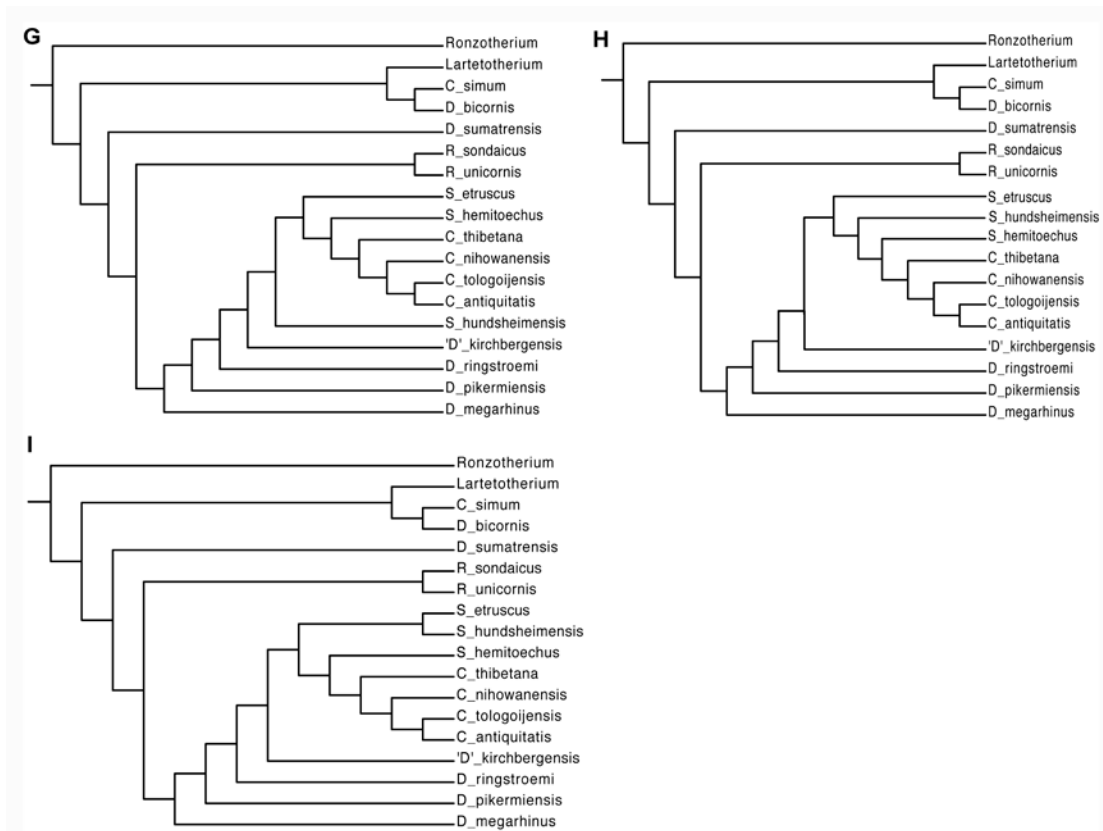
Fig. S7. Continued.

Fig. S8. Strict consensus of the 9 most parsimonious trees (Fig. S7). Decay values are above nodes and bootstrap frequencies below.
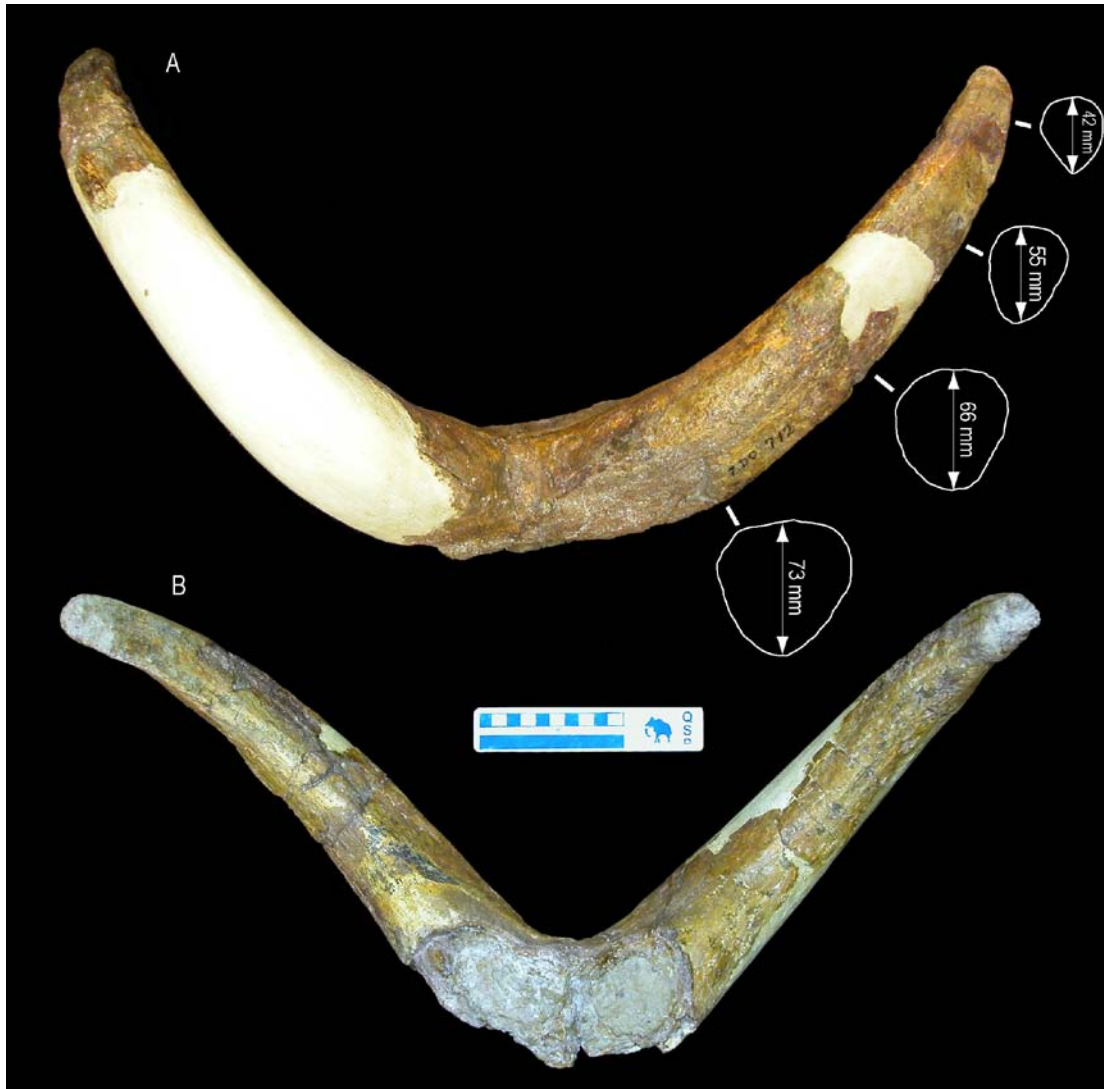
Fig. S9. 50% majority consensus of the 9 most parsimonious trees (Fig. S7).

Fig. S10. Occurrences of Rhinocerotidae in the NOW database (*87*) at Pliocene localities (aged between 2.59 and 5.31 Ma) of the Old World. There are a total of 229 reported occurrences in 173 localities, none of which include the genus *Coelodonta*.

Fig. S11. Horncore of ?*Pseudois* sp. from ZD0712 (~3.5 Ma), Zanda Basin, southwestern Tibet. A, dorsal view and cross-section outlines of horncore; B, posterior view of horncore. Scale = 10 cm.

Fig. S12. *Qurliqnoria* Bohlin from ZD0745 (~4.2 Ma), Zanda Basin, southwest Tibet. Relatively upright and straight (not posteriorly curved) and slightly divergent horncores with an oval cross-section are typical characters for this genus as well as the extant *Pantholops*, which has a more elongate and slender horncore. Anterior (A) and lateral (B) views of left horncore. Scale is in mm.
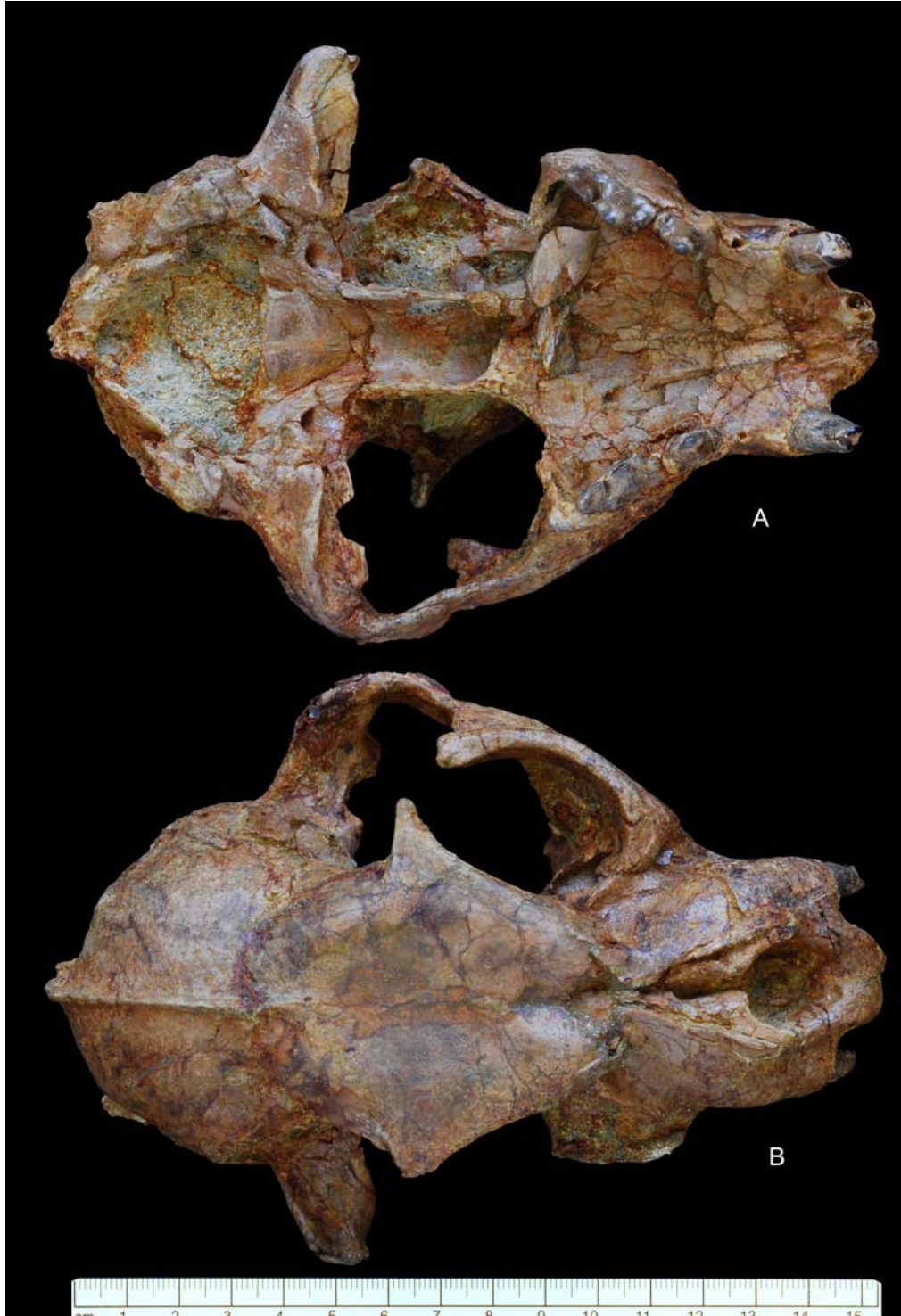
Fig. S13. A primitive snow leopard [*Panthera* (*Uncia*) sp.] from ZD1001 (~4.4 Ma), Zanda Basin, southwest Tibet. Somewhat smaller than extant snow leopard (*Panthera* (*Uncia*) *uncia*), the Zanda specimen displays a frontonasal compression and an expanded maxillary to the exclusion of jugal and lacrimal, features characteristic of the snow leopard. Ventral (A) and

dorsal (B) views of skull. Scale is in mm.

Tables in Supporting Online Material

Table S1. Composite list of vertebrate taxa from the Zanda strata (IVPP locality numbers in parentheses).

_____

Osteichthyes

      Cyprinidae

Mammalia

  Insectivora

      Soricidae indet. (ZD0609, 1001)

  Carnivora

      Nyctereutes cf. *N. tingi* (ZD0624)

      Vulpes sp. n. (ZD1001)

      Panthera (*Uncia*) sp. n. (ZD1001)

      Meles sp. n. (ZD1001, ZD1004)

      Mustela sp. (ZD1001)

      Chasmaporthetes sp. (ZD0908, 1029, 0636)

  Perissodactyla

      Hipparion zandaense (ZD0701 and others)

      Coelodonta thibetana new species (ZD0740)

  Artiodactyla

      Cervavitus sp. n. (ZD0624)

      ?*Pseudois* sp. n. (ZD0712)

      Antilospira/Spirocerus sp. (ZD0701, 1001)

      Qurliqnoria sp. (ZD0604, 0745)

      Bovidae gen. A (ZD1001)

      Bovidae gen. B (ZD1001)

  Proboscidea

      Gomphotheriidae indet. (ZD0746, 1015, 33, 36, 46, 48)

  Rodentia

      Aepyosciurus sp. (ZD1001)

      Nannocricetus sp. (ZD0609, 1001)

Cricetidae gen. et sp. nov. (ZD1001)

Prosiphneus cf. *P. eriksoni* (ZD1001)

Mimomys (*Aratomys*) *bilikeensis* (ZD0609, 0904)

Apodemus sp. (ZD0609, 0904)

Lagomorpha

Trischizolagus cf. *T. mirificus* (ZD0609, 0904)

Trischizolagus cf. *T. dumitrescuae* (ZD0726, 1001)

Ochotona sp. 1 (ZD0609, 0904)

Ochotona sp. 2 (ZD0609, 0902, 0904)

Ochotona sp. 3 (ZD1001)

Ochotona sp. 4 (ZD0726)

Table S2. Cranial measurements (in mm) of *Coelodonta thibetana*, as defined by Guérin (*55*).

Measures	*C. thibetana*	*C. nihowanensis*	*C. antiquitatis*
	V15908	HMV0980	Mean (Guérin, 1980)
1 Distance between occipital condyle and premaxillary tip	676	620	720.8
2 Distance between nasal tip and occipital condyle	692.2	650	720.8
3 Distance between nasal tip and occipital crest	771	770	781
4 Distance between the nasal tip and notch	224	200	205.2
5 Minimal width of the braincase	109	82.5	126.4
6 Distance between occipital crest and postorbital process	349	360	335.2
7 Distance between occipital crest and supraorbital tubercle	418	390	393.8
8 Distance between occipital crest and lacrimal tubercle	443	435	412.5
9 Distance between the nasal notch and the orbit	136	139	151.4
13 Distance between occipital condyle and M3	332	317	347.3
14 Distance between the nasal tip and the orbit	369	335	373.9
15 width of occipital crest	190	145	206.9
16 width between mastoid processes	225.2	212.5	273.1
17 Minimal width between the parietal crests	46.5	32	90.5
18 Width between postorbital processes	222.5	195	218.1
19 Width between supraorbital tubercles	~244	-	248.6
20 Width between lacrimal tubercles	~320	255	286.7
21 Maximal width between the zygomatic arches	303.4	294	334
22 Width of the nasal base	178	140	165.1
23 Height of occipital face	~130	152	175.2
25 Height of skull in front of P2	~153	171	196.1
26 Height of skull in front of M1	~123	178	195.6
27 Height of skull in front of M3	~140	190	206.8
28 Width of the palate in front of P2	~94	46	64.4
29 Width of the palate in front of M1	~90	64	87.7
30 Width of the palate in front of M3	~100	77	98
31 Width of foramen magnum	62.5	45	59.9
32 Width between occipital condyles	141.4	140	157.4

Table S3. Mandibular measurements (in mm) of *Coelodonta thibetana* as defined by Guérin (*55*).

Measures	*C. thibetana*	*C. nihowanensis*	*C. antiquitatis*
	V15908	HMV0980	Mean (Guérin, 1980)
1 Length	512	508	525.6
2 Distance between symphysis and angular process	415	435	425.6
3 Height of horizontal ramus in front of p3	87.6	73.5	81.6
4 Height of horizontal ramus in front of p4	89.8	80	88.5
5 Height of horizontal ramus in front of m1	97.4	95	96.8
6 Height of horizontal ramus in front of m2	97.7	102	101
7 Height of horizontal ramus in front of m3	96.2	107	100.9
8 Height of horizontal ramus posterior to m3	104.8	112	108.4
9 Distance between horizontal rami in front of m1	-	60	61.6
10 Distance between horizontal rami in front of m3	-	68	58
11 Length of symphysis	119	86	119.6
13 Antero-posterior diameter of ascending ramus	154	164	168.4
14 Transverse diameter of condyle	101.3	99.5	99.8
15 Height at condyle	269	268	263.8
16 Height at coronoid process	311	325	331.5

Table S4. Measurements of cheek teeth (in mm) of *Coelodonta thibetana* (length × width × height).

Upper teeth	V 15908	Lower teeth	V15908
P2	33.2×33.4×27.4	p2	27.5×17×22.5
P3	37.6×46.6×26.7	p3	32.9×25.1×25.5
P4	41×51.8×30.2	p4	38.2×27.1×31.3
M1	50×57.4×31.9	m1	39.7×29.8×28
M2	54.1×60.5×43.7	m2	45.9×29.7×34
M3	60.9×57.2×52.9	m3	47.3×30×35.2

Table S5. Measurements of atlas of *Coelodonta thibetana* (in mm).

Measures	V15908
Total length in projection, without ventral tubercle	>121
Width between alar notches	152
Distance between inferior alar foramina	149

Table S6. Measurements of axis and third cervical vertebrata of *Coelodonta thibetana* (in mm).

Measures	Axis	Third cervical vertebra
Length of body	115	85
Width of the caudal articular surface	49.4	49.7
Height of the caudal articular surface	63.6	65
Total height of vertebra	171	-
Width of cranial articulation	154	117
Width of caudal articulation	103.3	81
Minimum width of body	122	64.5
Length of arch in sagittal axis	77.6	36.3
Length of arch at the base	45.5	39.2
Maximum width between transverse processes	-	122

Table S7. Character list. Description of characters used in the phylogenetic analysis of Rhinocerotini. Characters 1-39 are from Antoine (*62*), characters 40-46 are new to this study. Character numbers from Antoine (*62*) (in brackets) follow the character numbers used in this study, and an asterisk (*) indicates a character has been modified from how it was used in Antoine (*62*).

Skull

1 (2) Maxillary infraorbital foramen = 0 above premolars; 1, above molars

2 (3) Nasal notch = 0, above P1-3; 1, above P4-M1

3 (4) Nasal septum = 0, never ossified; 1, ossified even sometimes

4 (5*) Nasal septum: ossified = 0, weakly; 1, strongly

5 (7) Orbit: anterior border = 0, above P4-M2; 1, above M3

6 (9) Frontal: postorbital process = 0, present; 1, absent

7 (10) Maxillary: anterior base of the maxillary zygomatic process = 0, high; 1, low

8 (11) Zygomatic arch = 0, low; 1, high

9 (15) Skull: dorsal profile = 0, flat; 1, concave; 2, very concave

10 (18) External auditory pseudo-meatus = 0, open; 1, closed

11 (19) Occipital side = 0, inclined forward; 1, vertical; 2, inclined backward

12 (20) Occipital nuchal tubercle = 0, little developed; 1, developed; 2, very developed

13 (21) Skull: back of teeth row = 0, in the posterior half; 1, restricted to the anterior half

14 (24) Nasal bones: rostral end = 0, narrow; 1, broad; 2, very broad

15 (31) Frontal horn = 0, absent; 1, = present

16 (33) Lateral projection of the orbit = 0, absent; 1, present

17 (35*) Frontal-parietal = 0, close frontoparietal crests; 1, distant crests

Mandible

18 (53) Symphysis = 0, very upraised; 1, upraised; 2, nearly horizontal

19 (59) Mandibular corpus: base = 0, straight; 1, convex; 2, very convex

20 (60) Ramus = 0, vertical; 1, inclined forward; 2, inclined backward

Teeth

21 (63) Compared length of the premolars/molars rows = 0, $100 \times L_{P3-4}/L_{M1-3} > 50$; 1, $42 < 100 \times L_{P3-4}/L_{M1-3} < 50$

22 (66*) Cheek teeth: cement = 0, absent; 1, weak or variable; 2, abundant

23 (68) Cheek teeth: crown = 0, low; 1, high

24 (69) Cheek teeth: crown = 0, high; 1, partial hypsodonty; 2, subhypsodonty; 3, hypsodonty

25 (71) I1 = 0, present; 1, absent

26 (78) i2 = 0, present; 1, absent

27 (91*) P1 in adults = 0, always present; 1, absent

28 (94) P2: protocone and hypocone = 0, fused; 1, lingual bridge; 2, separate; 3, lingual wall

29 (97) P2: protocone = 0, equal or stronger than the hypocone; 1, less strong than the hypocone

30 (113*) Upper molars: mediofossette = 0, absent; 1, present

31 (119) M1-2: metacone fold = 0, present; 1, absent

32 (122) M1-2: posterior part of the ectoloph = 0, straight; 1, concave

33 (134) M3: shape = 0, quadrangular; 1, triangular

34 (137) M3: protoloph = 0, transverse; 1, lingually elongated

35 (138) M3: posterior groove on the ectometaloph = 0, present; 1, absent

36 (142) Lower cheek teeth: trigonid = 0, angular; 1, rounded

37 (144*) Lower cheek teeth: metaconid = 0, not elongated; 1, elongated

38 (161) Lower molars: hypolophid = 0, transverse; 1, oblique; 2, almost sagittal

Postcrania

39 (279*) Limbs = 0, slender; 1, robust

Additional new characters

40 Skull: nasal tip to front of orbit / front of orbit to condyles = 0, < 75; 1, 75 - 90; 2, > 90

41 Nasal bones = 0, flat or evenly curved; 1, angled or with raised protuberance; 2, rostrally massive

42 Nasal bones: anterior end = 0, horizontal; 1, bent slightly downward; 2, bent strongly downward

43 Nasal horn: boss = 0, rounded; 1, narrow

44 Nasal horn: sagittal ridge on the boss = 0, absent; 1, present

45 Upper molars: lingual cusp bases = 0, not bulbous (inflated, swollen); 1, bulbous

46 Upper molars: occlusal topography = 0, ectolophodont; 1 = plagiolophodont

Table S8. Data matrix used in the phylogenetic analysis of Rhinocerotini. Modified from Antoine (*62*), including 18 taxa (one as outgroup) and 46 characters (see Table S7 for character description). Missing data coded as '?', inapplicable characters as '-'.

```
Character               1          2          3          4
Number          1234567890 1234567890 1234567890 1234567890 123456

Ronzotherium    100-000010 0000000000 0-0-000100 1000000000 010000
Lartetotherium  000-010021 1100111200 0-0-101110 1110100100 010000
D.sumatrensis   0010000010 0101101100 000-001210 1010110101 000000
R.sondaicus     0010000011 0101001201 000-001210 1010110100 000000
R.unicornis     0010000021 0101001201 0011001211 1011111100 110000
C.simum         000-110020 2202111022 0213111311 1001001200 210001
D.bicornis      000-011020 1212111021 0010111210 1010110100 200000
S.etruscus      0010001001 1001101101 0010111110 1110110101 110000
S.hundsheimensis 0010001001 1001101100 0010111110 1110110102 110000
S.hemitoechus   1110001111 2011101112 1112111110 1110110102 020000
D.ringstroemi   000-001011 1001101110 0010011100 1110110102 110010
D.pikermiensis  000-001011 1001101100 0010001110 0110110101 110010
D.megarhinus    000-101011 1001101100 0010001210 1110110100 010010
'D'.kirchbergensis 0010101011 1001101100 0011111210 1110110100 110010
C.thibetana     0110111101 2011101112 0111111311 01100101?0 111001
C.nihowanensis  0011000101 1011101122 0112111301 0111010100 111101
C.tologoijensis 00111?1001 2012101112 11121111?1 0101000201 011101
C.antiquitatis  1111111011 2012101122 1213111101 0001001211 021101
```

References

1. C. Guérin, La famille des Rhinocerotidae (Mammalia, Perissodactyla): Systématique, histoire, évolution, paléoécologie. *Cranium* **2**, 3 (1989).

2. D. R. Prothero, C. Guérin, E. Manning, in *The Evolution of Perissodactyls,* D. R. Prothero, R. M. Schoch, Eds. (Oxford Univ. Press, New York, 1989), pp. 321–340.

3. R.-D. Kahlke, F. Lacombat, The earliest immigration of woolly rhinoceros (*Coelodonta tologoijensis*, Rhinocerotidae, Mammalia) into Europe and its adaptive evolution in Palaearctic cold stage mammal faunas. *Quat. Sci. Rev.* **27**, 1951 (2008). doi:10.1016/j.quascirev.2008.07.013

4. T. Deng, Neogene rhinoceroses of the Linxia Basin (Gansu, China). *Cour. Forsch.- Inst. Senckenberg* **256**, 43 (2006).

5. L. Orlando *et al*., Ancient DNA analysis reveals woolly rhino evolutionary relationships. *Mol. Phylogenet. Evol.* **28**, 485 (2003). doi:10.1016/S1055-7903(03)00023-X Medline

6. Z.-x. Qiu, T. Deng, B. Y. Wang, Early Pleistocene mammalian fauna from Longdan, Dongxiang, Gansu, China. *Palaeontol. Sinica N. S. C* **27**, 1 (2004).

7. T. Deng, The earliest known woolly rhino discovered in the Linxia Basin, Gansu Province, China. *Geol. Bull. China* **21**, 604 (2002).

8. J. C. Zachos, G. R. Dickens, R. E. Zeebe, An early Cenozoic perspective on greenhouse warming and carbon-cycle dynamics. *Nature* **451**, 279 (2008). doi:10.1038/nature06588 Medline

9. F. E. Zeuner, Die Beziehungen zwischen Schädelform und Lebenweise bei den rezenten und fossilen Nashörnern. *Ber. Naturf. Ges. Freiburg.* **34**, 21 (1934).

10. I. X. Giaourtsakis, The late Miocene mammal faunas of the Mytilinii Basin, Samos Island, Greece: New collection. 9. Rhinocerotidae. Beitr. *Paläont.* **31**, 157 (2009).

11. J. E. Saylor *et al*., The late Miocene through present paleoelevation history of southwestern Tibet. *Am. J. Sci.* **309**, 1 (2009). doi:10.2475/01.2009.01

12. E. Haase, *Tiere der Verzeit* (Verlag von Quelle & Meyer, Leipzig, Germany, 1914).

13. M. Fortelius, The morphology and paleobiological significance of the horns of *Coelodonta antiquitatis* (Mammalia: Rhinocerotidae). *J. Vertebr. Paleontol.* **3**, 125 (1983). doi:10.1080/02724634.1983.10011964

14. N. Thew, L. Chaix, C. Guérin, in *La Faune*, D. Aubry, M. Guélat, J. Detrey, B. Othenin-Girard, Eds. (Cahier d'Archéologie Jurassienne, Porrentruy, Switzerland, 2000), pp. 93–98.

15. R.-D. Kahlke, *The History of the Origin, Evolution and Dispersal of the Late Pleistocene Mammuthus-Coelodonta Faunal Complex in Eurasia (Large Mammals)* (Fenske Companies, Rapid City, South Dakota, 1999).

16. E. A. Vangengeim, E. I. Beljaeva, V. Y. Garutt, E. L. Dmitrieva, V. S. Zazhigin, Eopleistocene mammals of Western Transbaikalia. *Trudy Geol. Inst. Akad. Nauk SSSR* **152**, 92 (1966).

17. G.-f. Zong, Q. Q. Xu, W. Y. Chen, Note on the late Pleistocene mammalian fossils in the Apa Zangzu Zizhizhou. Vert. *PalAsiat.* **23**, 161 (1985).

18. S.-h. Zheng, W.-y. Wu, Y. Li, Late Cenozoic mammalian faunas of Guide and Gonghe basins, Qinghai Province. *Vert. PalAsiat.* **23**, 89 (1985).

19. X. Wang *et al.*, Vertebrate paleontology, biostratigraphy, geochronology, and paleoenvironment of Qaidam Basin in northern Tibetan Plateau. *Palaeogeogr. Palaeoclimatol. Palaeoecol.* **254**, 363 (2007). doi:10.1016/j.palaeo.2007.06.007

20. H. R. Rezaei *et al.*, Evolution and taxonomy of the wild species of the genus *Ovis* (Mammalia, Artiodactyla, Bovidae). *Mol. Phylogenet. Evol.* **54**, 315 (2010). doi:10.1016/j.ympev.2009.10.037 Medline

21. A. Hassanin, A. Ropiquet, Molecular phylogeny of the tribe Bovini (Bovidae, Bovinae) and the taxonomic status of the Kouprey, *Bos sauveli* Urbain 1937. *Mol. Phylogenet. Evol.* **33**, 896 (2004). doi:10.1016/j.ympev.2004.08.009 Medline

22. N. K. Verestchagin, The Baikalian yak (*Phoephagus baikalensis* N. Ver. sp. nova, Mammalia) in Pleistocene fauna of eastern Siberia. *Dokl. Akad. Nauk SSSR* **99**, 455 (1954).

23. R.-D. Kahlke, The origin of Eurasian mammoth faunas. *Quarternaire, Horse-Série* **3**, 21 (2010).

24. P.-O. Antoine, Phylogénie et évolution des Elasmtheriina (Mammalia, Rhinocerotidae). *Mém. Mus. Natl. Hist. Nat.* **188**, 1 (2002).

25. M. A. Murphy, A. Yin, Structural evolution and sequence of thrusting in the Tethyan fold-thrust belt and Indus-Yalu suture zone, southwest Tibet. *Geol. Soc. Am. Bull.* **115**, 21 (2003). doi:10.1130/0016-7606(2003)115<0021:SEASOT>2.0.CO;2

26. M. A. Murphy *et al.*, Structural evolution of the Gurla Mandhata detachment system, southwest Tibet: Implications for the eastward extent of the Karakoram fault system. *Geol. Soc. Am. Bull.* **114**, 428 (2002). doi:10.1130/0016-7606(2002)114<0428:SEOTGM>2.0.CO;2

27. R. C. Thiede *et al.*, Dome formation and extension in the Tethyan Himalaya, Leo Pargil, northwest India. *Geol. Soc. Am. Bull.* **118**, 635 (2006). doi:10.1130/B25872.1

28. J. E. Saylor, thesis, Univ. of Arizona, Tucson, AZ (2008).

29. Q.-s. Zhang, F.-b. Wang, H.-x. Ji, W.-b. Huang, Pliocene stratigraphy of Zhada Basin, Tibet. *J. Stratigr.* **5**, 216 (1981).

30. D. Zhu *et al.*, Redefinition and redivision of the Pliocene-early Pleistocene lacustrine strata in Zanda basin, Ngari, Tibet, China. *Geol. Bull. China* **24**, 1111 (2005).

31. J. E. Saylor *et al.*, The late Miocene through present paleoelevation history of southwestern Tibet. *Am. J. Sci.* **309**, 1 (2009). doi:10.2475/01.2009.01m

32. S. Wang, W. Zhang, X. Fang, S. Dai, O. Kempf, Magnetostratigraphy of the Zanda basin in southwest Tibet Plateau and its tectonic implications. *Chin. Sci. Bull.* **53**, 1393 (2008). doi:10.1007/s11434-008-0132-9

33. F. Qian, Study on magnetostratigraphy in Qinghai-Tibetan plateau in late Cenozoic. *J. Geomech.* **5**, 22 (1999).

34. X. Meng *et al*., Discovery of rhinoceros fossils in the Pliocene in the Zanda basin, Ngari, Tibet. *Geol. Bull. China* **23**, 609 (2004).

35. X. Meng *et al*., Discovery of fossil teeth of Pliocene *Ochotona* in the Zanda basin, Ngari, Tibet, China. *Geol. Bull. China* **24**, 1175 (2005).

36. O. Kempf *et al*., Sedimentology, sedimentary petrology, and paleoecology of the monsoon-driven, fluvio-lacustrine Zhada Basin, SW-Tibet. *Sediment. Geol.* **222**, 27 (2009). doi:10.1016/j.sedgeo.2009.07.004

37. F.-l. Li, D.-l. Li, in *Paleontology of the Ngari Area, Tibet (Xi Zang)*, Z. Yang, Z. Nie, Eds. (China Univ. of Geological Science Press, Wuhan, China, 1990), pp. 186–193.

38. Z.-d. Qiu, G. Storch, The early Pliocene micromammalian fauna of Bilike, Inner Mongolia, China (Mammalia: Lipotyphla, Chiroptera, Rodentia, Lagomorpha). *Senckenbergiana Lethaea* **80**, 173 (2000).

39. C. A. Repenning, in *Vertebrate Fossils and Their Context, Contributions in Honor of Richard H. Tedford,* L. J. Flynn, Ed. (American Museum of Natural History, New York, 2003), vol. 279, pp. 469–512.

40. O. Fejfar, W.-D. Heinrich, M. A. Pevzner, E. A. Vangengeim, Late Cenozoic sequences of mammalian sites in Eurasia: An updated correlation. *Palaeogeogr. Palaeoclimatol. Palaeoecol.* **133**, 259 (1997). [doi:10.1016/S0031-0182(97)00085-0](doi:10.1016/S0031-0182(97)00085-0)

41. J. Chaline, P. Brunet-Lecomte, S. Montuire, L. Viriot, F. Courant, Anatomys of the arvicoline radiation (Rodentia): Paleogeographical, palaeoecological history and evolutionary data. *Ann. Zool. Fenn.* **36**, 239 (1999).

42. C. A. Repenning, in *Cenozoic Mammals of North America, Geochronology and Biostratigraphy*, M. O. Woodburne, Ed. (Univ. of California Press, Berkeley, CA, 1987), pp. 236–268.

43. C. J. Bell *et al*., in *Late Cretaceous and Cenozoic Mammals of North America: Biostratigraphy and Geochronology*, M. O. Woodburne, Ed. (Columbia Univ. Press, New York, 2004), pp. 232–314.

44. E. H. Lindsay *et al*., Recognition of the Hemphillian/Blancan boundary in Nevada. *J. Vertebr. Paleontol.* **22**, 429 (2002). [doi:10.1671/0272-4634(2002)022[0429:ROTHBB]2.0.CO;2](doi:10.1671/0272-4634(2002)022[0429:ROTHBB]2.0.CO;2)

45. L. Lourens, F. Hilgren, N. J. Shackleton, J. Laskar, J. Wilson, in *A Geologic Time Scale 2004*, F. M. Gradstein, J. G. Ogg, A. G. Smith, Eds. (Cambridge Univ. Press, Cambridge, 2004), pp. 409–440.

46. R. H. Tedford, Z.-x. Qiu, Pliocene *Nyctereutes* (Carnivora: Canidae) from Yushe, Shanxi, with comments on Chinese fossil raccoon-dogs. Vert. *PalAsiat.* **29**, 176 (1991).

47. Z.-x. Qiu, R. H. Tedford, A Pliocene species of *Vulpes* from Yushe, Shanxi. *Vert. PalAsiat.* **28**, 245 (1990).

48. Z.-x. Qiu, T. Deng, B. Y. Wang, Early Pleistocene mammalian fauna from Longdan, Dongxiang, Gansu, China. *Palaeontol. Sinica N. S. C* **27**, 1 (2004).

49. Z.-x. Qiu, Die hyaeniden aus dem Ruscinium und Villfranchium Chinas. Münchner Geowiss. *Abh.* **9**, 1 (1987).

50. T. Ringström, Nashörner der *Hipparion* Fauna Nord-Chinas. *Palaeontol. Sinica S. C* **1**, 1 (1924).

51. P. Mazza, The Tuscan early Pleistocene rhinoceros *Dicerorhinus etruscus*. Palaeontog. *Italica* **75**, 1 (1988).

52. G.-f. Chen, A new genus of Iranotheriinae of Ningxia. *Vert. PalAsiat.* **15**, 143 (1977).

53. T. Deng, New discovery of *Iranotherium morgani* (Perissodactyla, Rhinocerotidae) from the late Miocene of the Linxia Basin in Gansu, China, and its sexual dimorphism. *J. Vertebr. Paleontol.* **25**, 442 (2005). doi:10.1671/0272-4634(2005)025[0442:NDOIMP]2.0.CO;2

54. T. Deng, Skull of *Parelasmotherium* (Perissodactyla, Rhinocerotidae) from the upper Miocene in the Linxia Basin (Gansu, China). *J. Vertebr. Paleontol.* **27**, 467 (2007). doi:10.1671/0272-4634(2007)27[467:SOPPRF]2.0.CO;2

55. C. Guérin, Les rhinocéros (Mammalia, Perissodactyla) du Miocène terminal au Pléistocène supérieur en Europe occidentale: comparaison avec les espèces actuelles. *Doc. Lab. Géol. Lyon* **79**, 1 (1980).

56. J. C. Zachos, G. R. Dickens, R. E. Zeebe, An early Cenozoic perspective on greenhouse warming and carbon-cycle dynamics. *Nature* **451**, 279 (2008). doi:10.1038/nature06588 Medline

57. R.-D. Kahlke, F. Lacombat, The earliest immigration of woolly rhinoceros (*Coelodonta tologoijensis*, Rhinocerotidae, Mammalia) into Europe and its adaptive evolution in Palaearctic cold stage mammal faunas. *Quat. Sci. Rev.* **27**, 1951 (2008). doi:10.1016/j.quascirev.2008.07.013

58. T. Deng, Neogene rhinoceroses of the Linxia Basin (Gansu, China). Cour. Forsch.-*Inst. Senckenberg* **256**, 43 (2006).

59. H. Loose, Pleistocene Rhinocerotidae of W. Europe with reference to the recent two-horned species of Africa and S.E. Asia. *Scripta Geol.* **33**, 1 (1975).

60. M. Borsuk-Bialynicka, Studies on the Pleistocene rhinoceros *Coelodonta antiquitatis* (Blumenbach). Palaeontol. *Polonica* **29**, 1 (1973).

61. P. Teilhard de Chardin, Fossil mammals from Locality 9 of Choukoutien. *Palaeontol. Sinica S. C* **7**, 1 (1936).

62. P.-O. Antoine, Phylogénie et évolution des Elasmtheriina (Mammalia, Rhinocerotidae). *Mém. Mus. Natl. Hist. Nat.* **188**, 1 (2002).

63. P. Teilhard de Chardin, J. Piveteau, Les mammifères fossiles de Nihowan (Chine). *Ann. Paleontol.* **19**, 1 (1930).

64. E. A. Vangengeim, E. I. Beljaeva, V. Y. Garutt, E. L. Dmitrieva, V. S. Zazhigin, Eopleistocene mammals of Western Transbaikalia. *Trudy Geol. Inst. Akad. Nauk SSSR* **152**, 92 (1966).

65. D. L. Swofford, *PAUP*: Phylogenetic Analysis Using Parsimony (*and other methods). Version 4.0b10*. (Sinauer, Sunderland, MA, 2002).

66. M. D. Sorenson, *TreeRot, version 2*. (Boston Univ., Boston, MA, 1999).

67. C. Tougard, T. Delefosse, C. Hänni, C. Montgelard, Phylogenetic relationships of the five extant Rhinoceros species (Rhinocerotidae, Perissodactyla) based on mitochondrial cytochrome *b* and 12S rRNA genes. *Mol. Phyl. Evol.* **19**, 34 (2001). doi:10.1006/mpev.2000.0903 Medline

68. E. Willerslev *et al.*, Analysis of complete mitochondrial genomes from extinct and extant rhinoceroses reveals lack of phylogenetic resolution. *BMC Evol. Biol.* **9**, 95 (2009). doi:10.1186/1471-2148-9-95 Medline

69. C. P. Groves, Phylogeny of the living species of Rhinoceros. *Sond. Z. Zool. Syst. Evol.* **21**, 293 (1983). doi:10.1111/j.1439-0469.1983.tb00297.x

70. D. R. Prothero, E. Manning, C. B. Hanson, The phylogeny of the Rhinocerotoidea (Mammalia, Perissodactyla). *Zool. J. Linn. Soc.* **87**, 341 (1986). doi:10.1111/j.1096-3642.1986.tb01340.x

71. E. Cerdeño, Cladistic analysis of the Family Rhinocerotidae (Perissodactyla). *Am. Mus. Novit.* **3143**, 1 (1995).

72. T. Deng, A new elasmothere (Perissodactyla, Rhinocerotidae) from the late Miocene of the Linxia Basin in Gansu, China. *Geobios* **41**, 719 (2008). doi:10.1016/j.geobios.2008.01.006

73. M. Fortelius, P. Mazza, B. Sala, *Stephanorhinus* (Mammalia: Rhinocerotidae) of the Western European Pleistocene, with a revision of *S. etruscus* (Falconer 1868). Palaeontog. *Italica* **80**, 63 (1993).

74. J. Jernvall, M. Fortelius, Common mammals drive the evolutionary increase of hypsodonty in the Neogene. *Nature* **417**, 538 (2002). doi:10.1038/417538a Medline

75. C. M. Janis, in *Body Size in Mammalian Paleobiology,* J. Damuth, B. J. MacFadden, Eds. (Cambridge Univ. Press, Cambridge, 1990), pp. 255–299.

76. C. M. Janis, The evolutionary strategy of the Equidae and the origins of rumen and cecal digestion. *Evolution* **30**, 757 (1976). doi:10.2307/2407816

77. M. Fortelius, Ungulate cheek teeth: Developmental, functional and evolutionary interrelations. *Acta Zool. Fenn.* **180**, 1 (1985).

78. M. Fortelius, N. Solounias, Functional characterization of ungulate molars using the abrasion-attrition wear gradient: A new method for reconstructing paleodiets. *Am. Mus. Novit.* **3301**, 1 (2000). doi:10.1206/0003-0082(2000)301<0001:FCOUMU>2.0.CO;2

79. T. E. Cerling *et al.*, Global vegetation change through the Miocene/Pliocene boundary. *Nature* **389**, 153 (1997). doi:10.1038/38229

80. M. J. Kohn, J. Law, Stable isotope chemistry of fossil bone as a new paleoclimate indicator. *Geochim. Cosmochim. Acta* **70**, 931 (2006). doi:10.1016/j.gca.2005.10.023

81. Y. Wang *et al.*, Stable isotopic variations in modern herbivore tooth enamel, plants and water on the Tibetan Plateau: Implications for paleoclimate and paleoelevation reconstructions. *Palaeogeogr. Palaeoclimatol. Palaeoecol.* **260**, 359 (2008). doi:10.1016/j.palaeo.2007.11.012

82. A. Zanazzi, M. J. Kohn, B. J. MacFadden, D. O. Terry, Large temperature drop across the Eocene-Oligocene transition in central North America. *Nature* **445**, 639 (2007). doi:10.1038/nature05551 Medline

83. M. H. O'Leary, Carbon isotopes in photosynthesis. *Bioscience* **38**, 328 (1988). doi:10.2307/1310735

84. M. J. Kohn, T. E. Cerling, in *Phosphates—Geochemical, Geobiological, and Materials Importance*, M. Kohn, J. Rakovan, J. Hughes, Eds. (Mineralogical Society of America, Washington, DC, 2002), vol. 48, pp. 455–488.

85. N. E. Levin, T. E. Cerling, B. H. Passey, J. M. Harris, J. R. Ehleringer, A stable isotope aridity index for terrestrial environments. *Proc. Natl. Acad. Sci. U.S.A.* **103**, 11201 (2006). doi:10.1073/pnas.0604719103 Medline

86. M. Fortelius, Neogene of the Old World Database of Fossil Mammals (NOW) (Univ. of Helsinki, Helsinki, Finland; www.helsinki.fi/science/now/, accessed 7 July 2011).

87. R. S. Hoffmann, in *Mammals of the Palaearctic Desert: Status and Trends in the Sahara-Gobi Region*, J. A. McNeely, V. Neronov, Eds. (Russian Academy of Sciences, Moscow, 1991), pp. 285–297.

88. R. S. Hoffmann, in *Fifth International Theriological Congress* (International Theriological Congress, Rome, 1989), vol. 2, p. 738.

89. S. J. Olsen, Fossil ancestry of the yak, its cultural significance and domestication in Tibet. *Proc. Acad. Nat. Sci. Philadelphia* **142**, 73 (1990).

90. N. K. Verestchagin, The Baikalian yak (*Phoephagus baikalensis* N. Ver. sp. nova, Mammalia) in Pleistocene fauna of eastern Siberia. *Dokl. Akad. Nauk SSSR* **99**, 455 (1954).

91. J. G. M. Thewissen *et al.*, Fossil yak (*Bos grunniens*: Artiodactyla, Mammalia) from the Himalayas of Pakistan. *Kirtlandia* **50**, 11 (1997).

92. A. Hassanin, A. Ropiquet, Molecular phylogeny of the tribe Bovini (Bovidae, Bovinae) and the taxonomic status of the Kouprey, *Bos sauveli* Urbain 1937. *Mol. Phyl. Evol.* **33**, 896 (2004). doi:10.1016/j.ympev.2004.08.009 Medline

93. A. Hassanin, E. J. P. Douzery, Evolutionary affinities of the enigmatic saola (*Pseudoryx nghetinhensis*) in the context of the molecular phylogeny of Bovidae. *Proc. Biol. Sci.* **266**, 893 (1999). doi:10.1098/rspb.1999.0720 Medline

94. C. Pitra, R. Fürbass, H. M. Seyfert, Molecular phylogeny of the tribe Bovini (Mammalia: Artiodactyla): alternative placement of the Anoa. *J. Evol. Biol.* **10**, 589 (1997). doi:10.1007/s000360050043

95. M. M. Miyamoto, S. M. Tanhauser, P. J. Laipis, Systematic relationships in the artiodactyl tribe Bovini (Family Bovidae), as determined from mitochondrial DNA sequences. *Syst. Biol.* **38**, 342 (1989).

96. M. Hernández Fernández, E. S. Vrba, A complete estimate of the phylogenetic relationships in Ruminantia: A dated species-level supertree of the extant ruminants. *Biol. Rev. Camb. Philos. Soc.* **80**, 269 (2005). doi:10.1017/S1464793104006670 Medline

97. D. M. Leslie, G. B. Schaller, *Bos grunniens* and *Bos mutus* (Artiodactyla: Bovidae). *Mamm. Species* **836**, 1 (2009).

98. C. P. Groves, Systematic relationships in the Bovini (Artiodactyla, Bovidae). *J. Zoological Syst. Evol. Res.* **19**, 264 (1981). [doi:10.1111/j.1439-0469.1981.tb00243.x](doi:10.1111/j.1439-0469.1981.tb00243.x)

99. T. D. Bunch, C. Wu, Y.-P. Zhang, S. Wang, Phylogenetic analysis of snow sheep (*Ovis nivicola*) and closely related taxa. *J. Hered.* **97**, 21 (2006). doi:10.1093/jhered/esi127 Medline

100. H. R. Rezaei *et al.*, Evolution and taxonomy of the wild species of the genus *Ovis* (Mammalia, Artiodactyla, Bovidae). *Mol. Phyl. Evol.* **54**, 315 (2010). doi:10.1016/j.ympev.2009.10.037 Medline

101. A. K. Fedosenko, D. A. Blank, Ovis ammon. *Mamm. Species* **773**, 1 (2005). [doi:10.1644/1545-1410(2005)773[0001:OA]2.0.CO;2](doi:10.1644/1545-1410(2005)773[0001:OA]2.0.CO;2)

102. F. Rivals, B. Deniaux, Dental microwear analysis for investigating the diet of an argali population (*Ovis ammon antiqua*) of mid-Pleistocene age, Caune de l'Arago cave, eastern Pyrenees, France. *Palaeogeogr. Palaeoclimatol. Palaeoecol.* **193**, 443 (2003). [doi:10.1016/S0031-0182(03)00260-8](doi:10.1016/S0031-0182(03)00260-8)

103. C. R. Harington, F. V. Clulow, Pleistocene mammals from Gold Run Creek, Yukon Territory. *Can. J. Earth Sci.* **10**, 697 (1973). [doi:10.1139/e73-069](doi:10.1139/e73-069)

104. C. R. Harington, Pleistocene mammals from Lost Chicken Creek, Alaska. *Can. J. Earth Sci.* **17**, 168 (1980). [doi:10.1139/e80-015](doi:10.1139/e80-015)

105. V. Eisenmann, in *Equids in the Ancient World*, R. H. Meadow, H.-P. Uerpmann, Eds. (Ludwig Reichert Verlag, Wiesbaden, Germany, 1986), pp. 67–116.

106. A. Forstén, Chinese fossil horses of the genus *Equus*. *Acta Zool. Fenn.* **181**, 1 (1986).

107. A. Forstén, A review of *Equus stenonis* Cocchi (Perissodactyla, Equidae) and related forms. *Quat. Sci. Rev.* **18**, 1373 (1999). [doi:10.1016/S0277-3791(98)00073-0](doi:10.1016/S0277-3791(98)00073-0)

108. A. Forstén, Mitochondrial-DNA time-table and the evolution of *Equus*: Comparison of molecular and paleontological evidence. *Ann. Zool. Fenn.* **28**, 301 (1992).

109. X. Wang, R. S. Hoffmann, Pseudois nayaur and Pseudois schaeferi. *Mamm. Species* **278**, 1 (1987). [doi:10.2307/3503993](doi:10.2307/3503993)

110. R. B. Harris, D. J. Miller, Overlap in summer habitats and diets of Tibetan Plateau ungulates. *Mammalia* **59**, 197 (1995). doi:10.1515/mamm.1995.59.2.197

111. B. Bohlin, Einige Jungtertiäre und Pleistozäne caviconnier aus Nord-China. *Nova Acta Regiae Societatis Scientiarum Upsaliensis, Series IV* **11**, 1 (1938).

112. Z.-j. Xu, thesis, Institute of Vertebrate Paleontology and Paleoanthropology, Beijing, China (2009).

113. P. Teilhard de Chardin, W.-c. Pei, The fossil mammals from locality 13 of Choukoutien. *Palaeontologia Sinica* **11**, 1 (1941) (series C).

114. T. D. Bunch, S. Wang, Y. Zhang, A. Liu, S. Lin, Brief communication. Chromosome evolution of the blue sheep/bharal (*Pseudois nayaur*). *J. Hered.* **91**, 168 (2000). doi:10.1093/jhered/91.2.168

115. L.-r. Cao, X.-m. Wang, S.-g. Fang, A molecular phylogeny of Bharal and dwarf blue sheep based on mitochondrial cytochrome b gene sequences. *Acta Zool. Sinica* **49**, 198 (2003).

116. A. W. Gentry, The extinct bovid genus *Qurliqnoria* Bohlin. *J. Mammal.* **49**, 769 (1968). doi:10.2307/1378744

117. X. Wang *et al.*, Vertebrate paleontology, biostratigraphy, geochronology, and paleoenvironment of Qaidam Basin in northern Tibetan Plateau. *Palaeogeogr. Palaeoclimatol. Palaeoecol.* **254**, 363 (2007). doi:10.1016/j.palaeo.2007.06.007

118. R. Lydekker, On the skull of a chiru-like antelope from the ossiferous deposits of Hundes (Tibet). *Q. J. Geol. Soc.* **57**, 289 (1901). doi:10.1144/GSL.JGS.1901.057.01-04.22

119. X. Wang, Z.-d. Qiu, Q. Li, Y. Wang, J. Tseng, A new vertebrate fauna in late Pliocene of Kunlun Mountain Pass, northern Tibetan Plateau and its paleoenvironmental implications. *J. Vertebr. Paleontol.* **26**, 136A (2006).

120. X. Wang *et al.*, in *Second International Palaeontological Congress*, Q. Yang, Y. Wang, E. A. Weldon, Eds. (Univ. of Science and Technology of China Press, Beijing, 2006), vol. T15–20, p. 470.

121. B. Kurtén, An attempted parallelization of the Quaternary mammalian faunas of China and Europe. *Societas Scientiarum Fennica Commentationes Biologicae* **23**, 1 (1960).

122. E. Thenius, Zur Kenntnis jungpleistozäner Feliden Mitteleuropas. Säugetierk. *Mitt.* **5**, 1 (1957).

123. E. Thenius, Über das Vorkommen fossiler Schneeleoparden (Subgenus *Uncia*, Carnivora, Mammalia). Säugetierk. *Mitt.* **17**, 234 (1969).

124. W.-z. Pei, On the Carnivora from Locality 1 of Choukoutien. *Palaeontologia Sinica* **8**, 1 (1934) (series C).

125. H. Hemmer, Untersuchungen zur Stammesgeschichte der Pantherkatzen (Pantherinae). Teil II: Studien zur Ethologie des Nebelparders *Neofelis nebulosa* (Griffith 1821) und des Irbis *Uncia uncia* (Schreber 1775). *Veröff. Zool. Staatssammlung München* **12**, 155 (1968).

126. H. Hemmer, Zur Kenntnis pleistozäne mittel europäischer Leoparden (*Panthera pardus*). *N. Jb. Geol. Paläont. Abh.* **138**, 15 (1971).

127. H. Hemmer, Uncia uncia. *Mamm. Species* **20**, 1 (1972). doi:10.2307/3503882

128. R. W. Dennell, R. Coard, A. Turner, Predators and scavengers in Early Pleistocene southern Asia. *Quat. Int.* **192**, 78 (2008). doi:10.1016/j.quaint.2007.06.023

129. R. W. Dennell, A. Turner, R. Coard, M. Beech, M. Anwar, Two upper Siwalik (Pinjor Stage) fossil accumulations from localities 73 and 362 in the Pabbi Hills, Pakistan. *Journal of the Palaeontological Society of India* **50**, 101 (2005).

130. L. O. Salles, Felid phylogenetics: Extant taxa and skull morphology (Felidae, Aeluroidea). *Am. Mus. Novit.* **3047**, 1 (1992).